SRM VALLIAMMAI ENGINEERING COLLEGE

(An Autonomous Institution)

SRM NAGAR, KATTANKULATHUR

DEPARTMENT OF ELECTRICAL & ELECTRONICS ENGINEERING

LAB MANUAL

M.E (POWER SYSTEMS ENGINEERING)

II Semester

PS3264 ADVANCED POWER SYSTEM SIMULATION LABORATORY

Regulation 2023

Academic Year 2024-2025 EVEN

Prepared by

Ms.S.Vanila, AP(Sel.G) /EEE

PS3264 ADVANCED POWER SYSTEM SIMULATION LABORATORY

SYLLABUS

1. Performance Characteristics of solar PV panel
2. Performance of PV panel in series and parallel combination
3. VI Characteristics of fuel cell.
4. Performance Characteristics of self – excited Induction Generator
5. Performance Characteristics of DFIG
6. Performance Characteristics of PMSG
7. MPPT tracking of DFIG based WT
8. MPPT tracking of PMSG based WT
9. Grid Integration of RES
10. Modeling of Active filter for Power system

PS3264 ADVANCED POWER SYSTEM SIMULATION LABORATORY

CYCLE – I

1. Performance Characteristics of solar PV panel
2. Performance of PV panel in series and parallel combination
3. VI Characteristics of fuel cell.
4. Performance Characteristics of self – excited Induction Generator
5. Performance Characteristics of DFIG

CYCLE – II

6. Performance Characteristics of PMSG
7. MPPT tracking of DFIG based WT
8. MPPT tracking of PMSG based WT
9. Grid Integration of RES
10. Modeling of Active filter for Power system

ADDITIONAL EXPERIMENTS

11. Simulation study on Hybrid (Solar-Wind) Power System.
12. Simulation study on Intelligent Controllers for Hybrid Systems.

INDEX

S.No	Date	Name of the Experiment	Marks	Signature

Ex. No.1
Date: **Performance Characteristics of solar PV panel**

AIM:

To conduct experiment on Performance assessment of Grid connected and Standalone 1kWp Solar Power System.

THEORY:

Photovoltaic (PV) power generation is a reliable and economical source of electricity in rural areas. It is important to operate the PV energy conversion systems near the maximum power point (MPP) to increase the efficiency of the PV system. But the solar energy always varies instantaneously and the current and power of PV array varies non-linearly with the terminal voltage, solar radiation, and temperature. So, the maximum power output cannot be easily obtained. As solar photovoltaic cells have significant nonlinear output characteristic, the photoelectric conversion efficiency is still very low. Therefore, so far the research of output characteristics of photovoltaic cells is an important topic in the industry. This paper proposes a mathematical model of PV array based on the principle of photovoltaic cells and establish the simulation model in Simulink. The output characteristic curve of the photovoltaic cells is obtained with different solar radiation and temperature. Thus, it can lay the foundation for in the following research of the maximum power point tracking.

PROCEDURE:

1. MATLAB Simulink model file is created.
2. Using Simulink library pv model generated.
3. Scope is verified for different values of V&I values.

SIMULATION DIAGRAM:

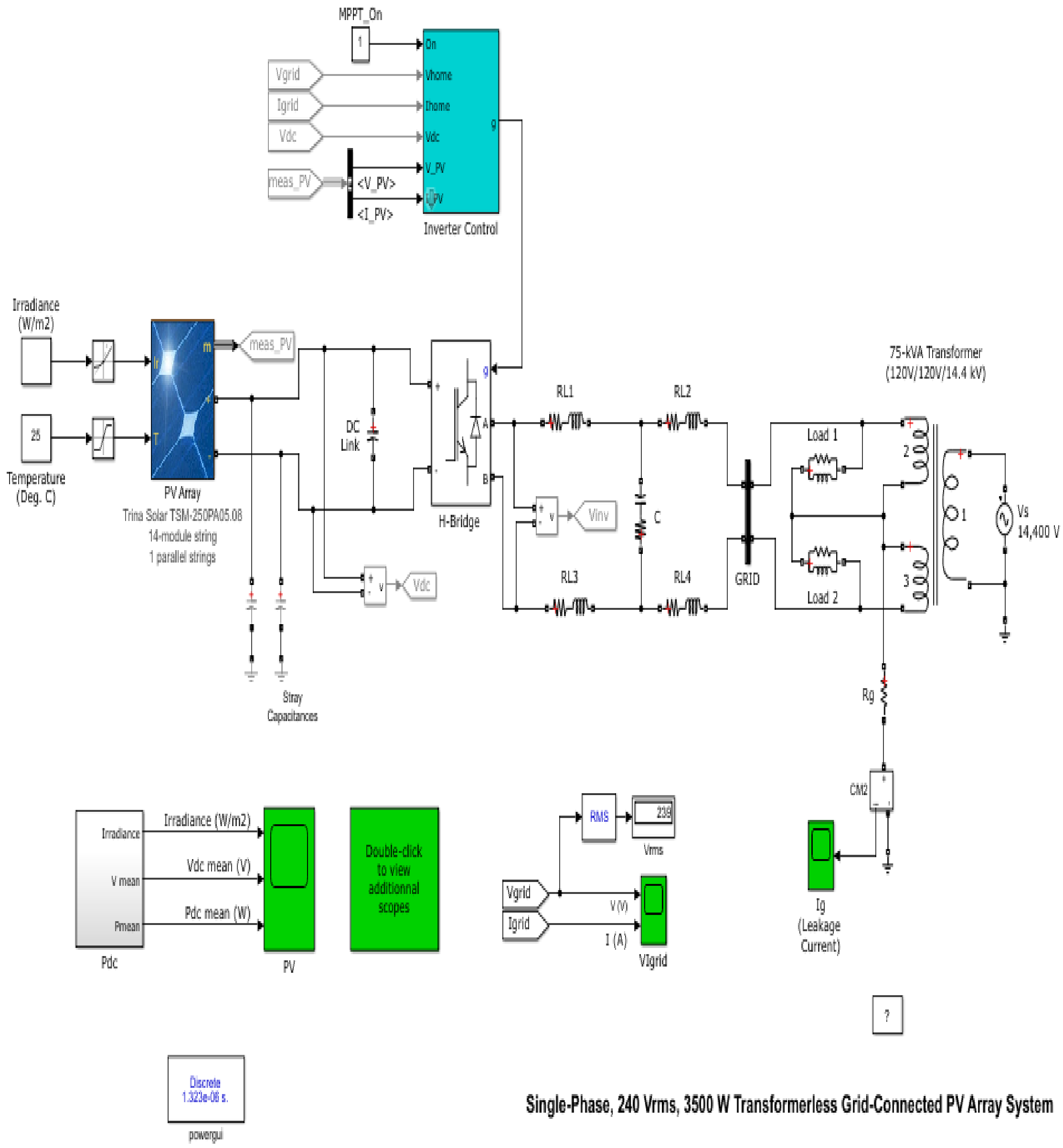

OUTPUT:

PV INPUT

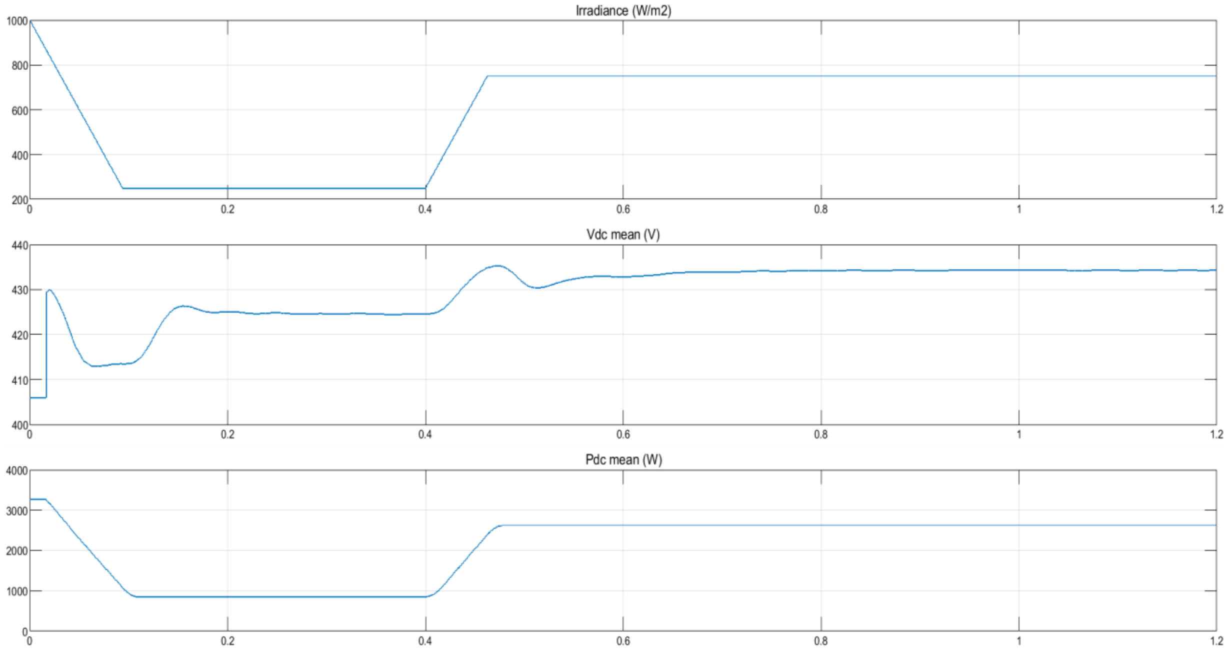

Voltage and Current

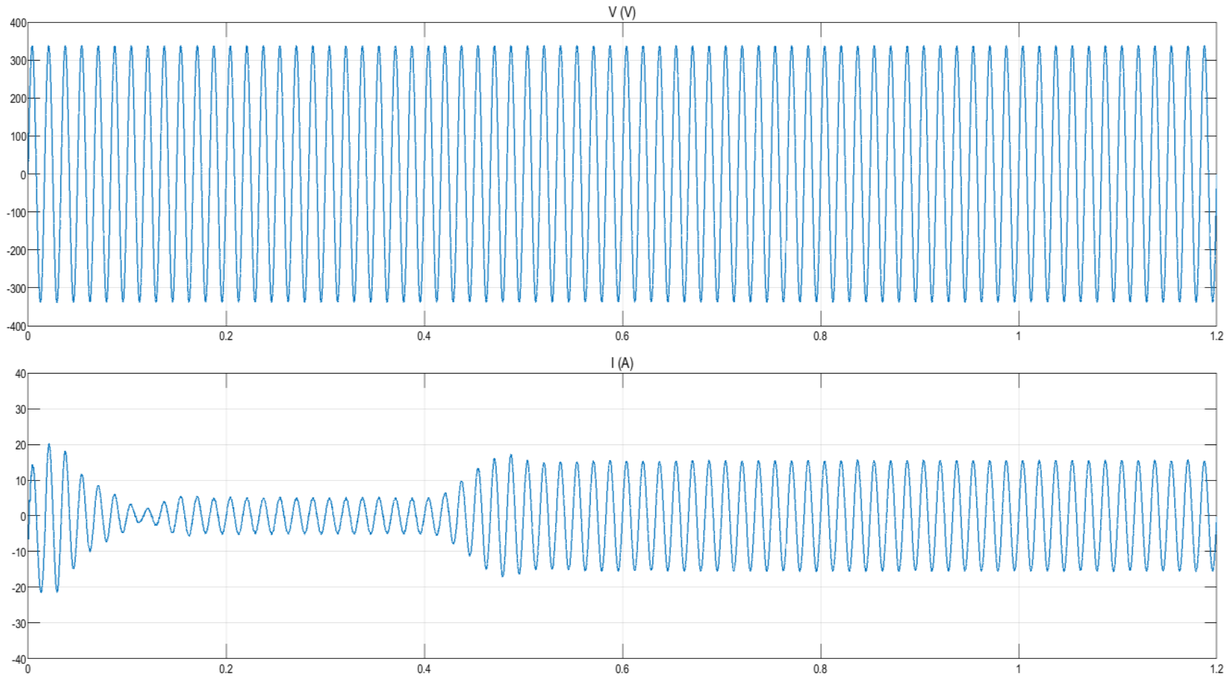

RESULT:

Thus, study of simulation of PV systems using MATLAB Simulink model was completed.

Ex.No: 2 Performance of PV panel in series and parallel combination

Date:

AIM:

To study the performance of PV panel in series and parallel combination using MATLAB Simulink software.

THEORY:

Solar cells are devices used to realize a direct conversion of sunlight energy into electricity by means of a viable technology known as photovoltaic (PV) technology. In order to obtain a desired voltage and current, solar panels are made from series and parallel combinations of solar cells. The maximum power from a solar panel can only be extracted when the internal resistance of the panel is equal to the load resistance.

SERIES CONNECTION:

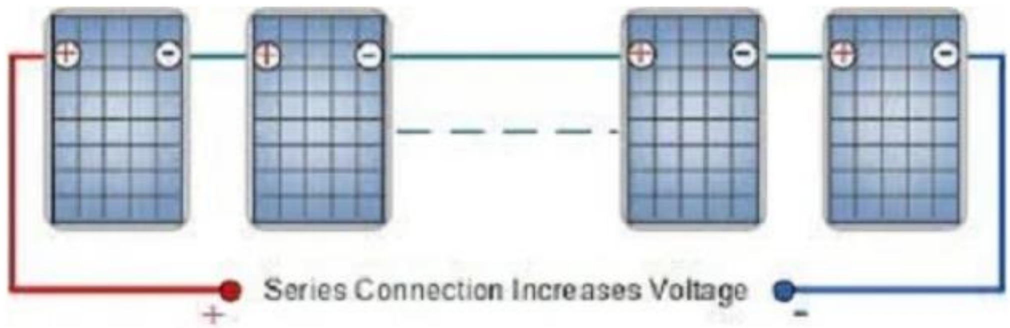

Figure 1: Solar panels connected in series.

$$V_{series} = V_1 + V_2 + V_3 + V_4$$

PARALLEL CONNECTION:

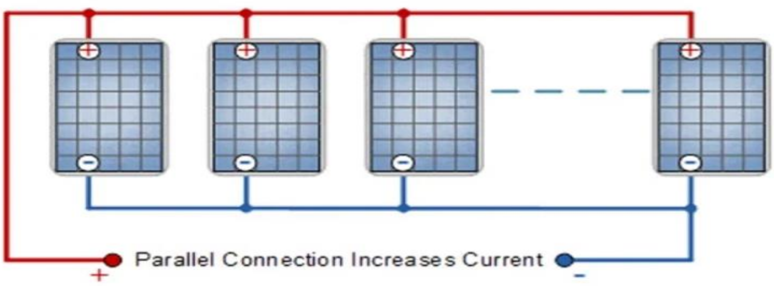

Figure 2: Solar panels connected in parallel.

$$I_{parallel} = I_1 + I_2 + I_3 + I_4$$

SERIES-PARALLEL CONNECTION:

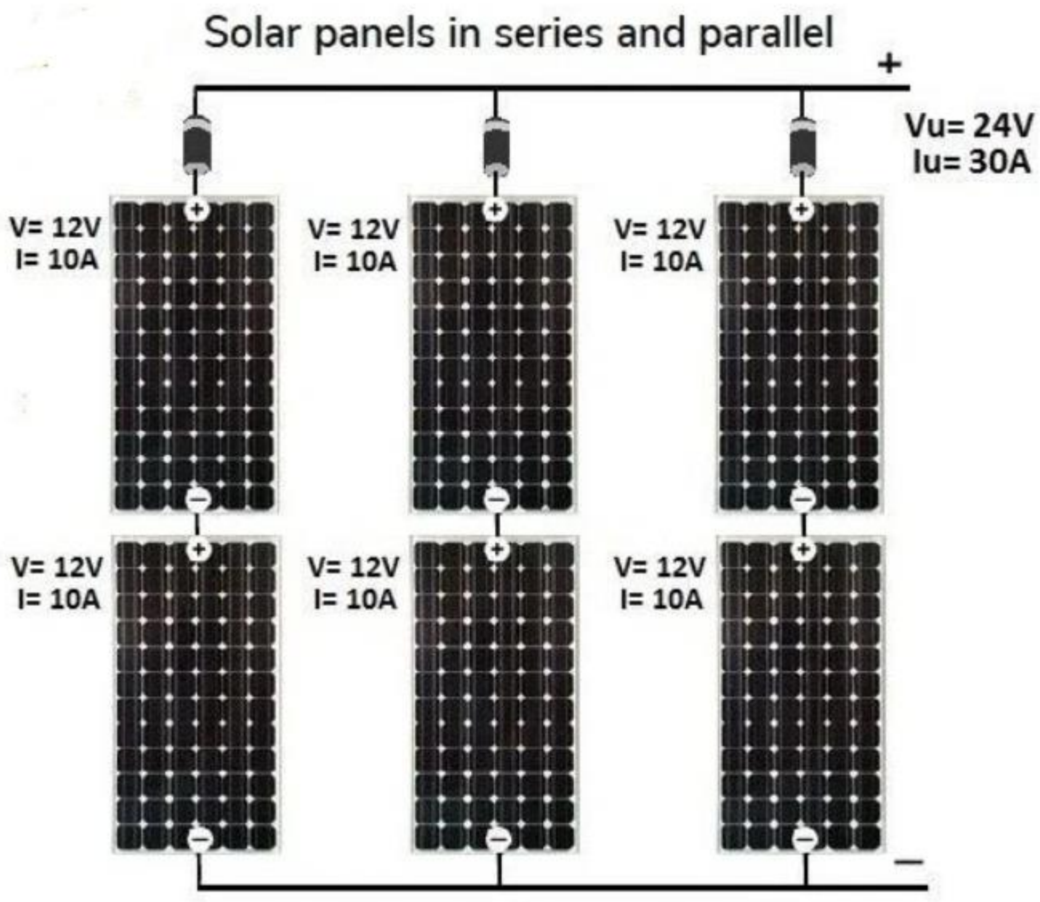

The series-parallel array configuration is the most commonly used configuration in most of the applications because it is easy to construct, economical and there are no redundant connections. Here, the PV modules are first connected in series connection to form strings to get a desired output voltage, and then these strings are connected in parallel to get desired output current. The MATLAB/Simulink model of 5 × 5 Series- Parallel PV array configurations is shown in Figure. This configuration comprises five parallel connected strings and each string consists of five series connected modules. In this configuration, the PV array current is the sum of the five individual string currents and the array voltage is equal to the sum of the individual module voltages in a string and the voltages across all the strings are same. In addition to bypass diodes, blocking diodes are connected in series to each PV string, to protect from severe PSCs or short circuit conditions. These diodes block reverse of string current into another string due to the potential difference between the strings under PSCs. In standalone PV systems, blocking diodes are preferred to block reverse flow of string current from the storage battery to PV array under PSCs or at night times.

The I-V and P-V characteristics of Series-Parallel PV array configuration under various shading conditions are shown in Figure. The advantages of Series-Parallel PV array configuration are, it performs better than Total-Cross-Tied configuration under row-wise shading and it is vulnerable to aging of PV modules. The limitations of this configuration are; it generates higher number of MPPs under PSCs and the performance is lower than the cross-tie configurations.

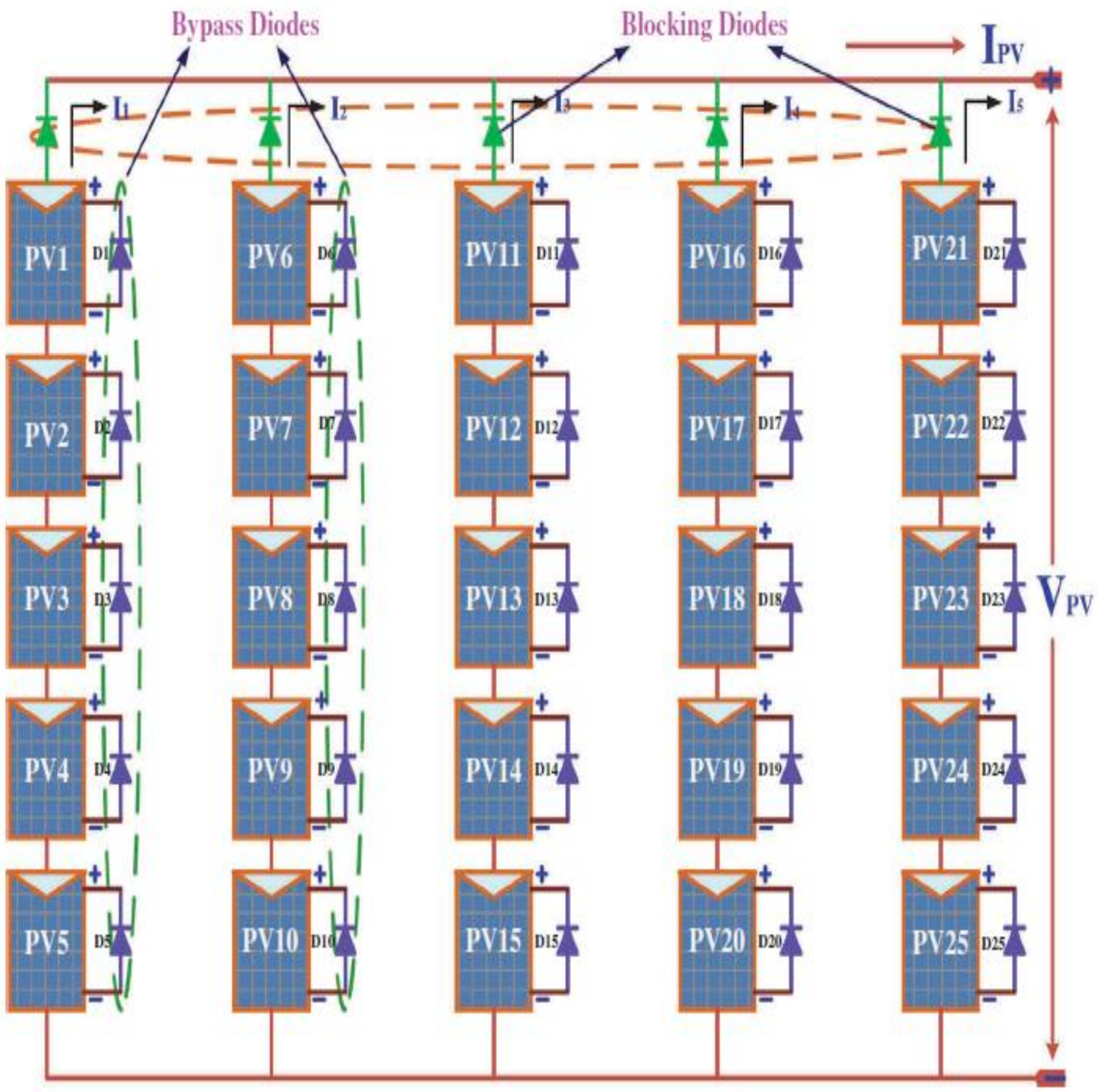

Series-Parallel PV array configuration

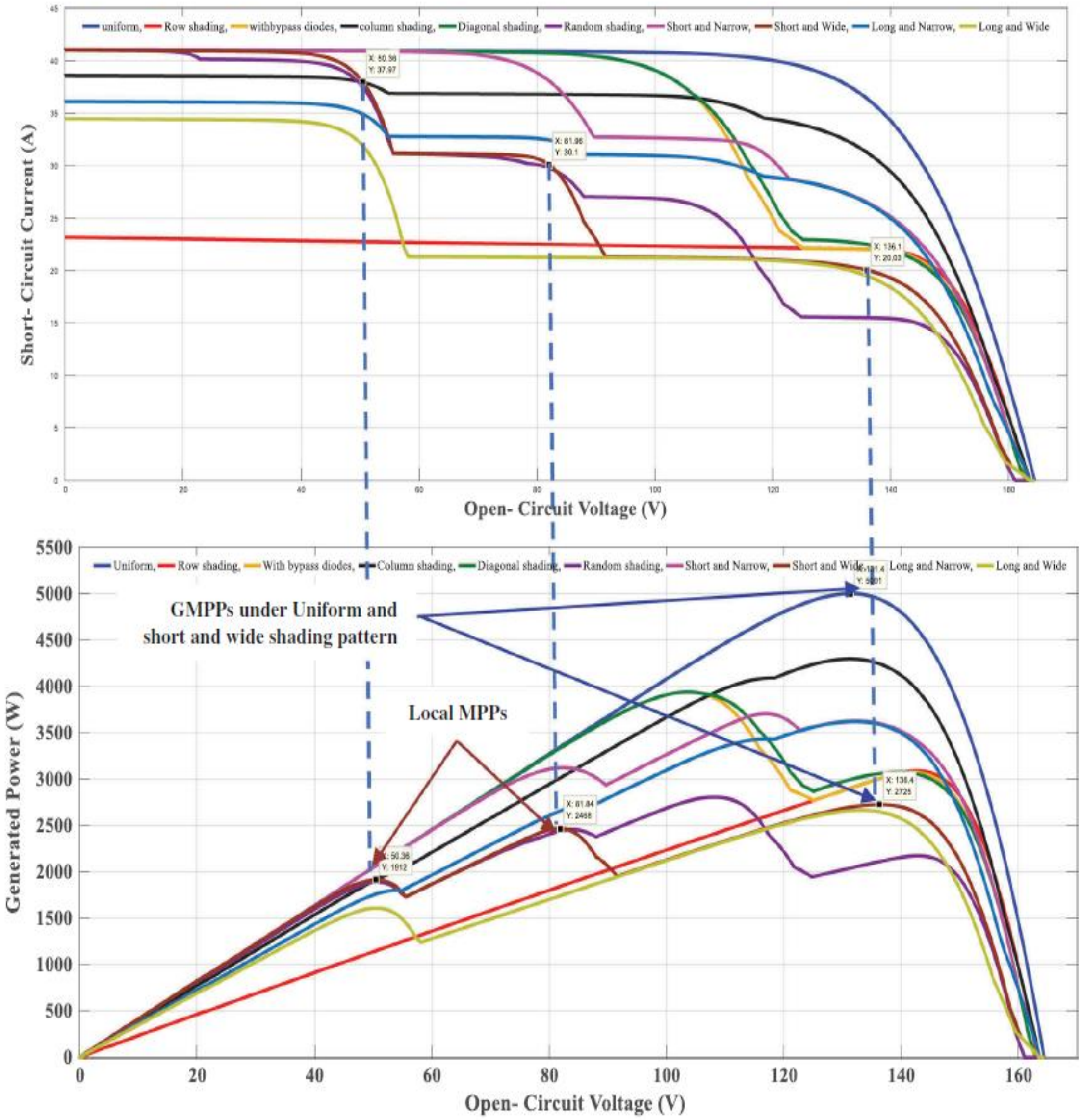

Simulated output characteristics (I-V and P-V) of Serial- Parallel configuration.

RESULT:

Thus the performance of PV panel in series and parallel combination using MATLAB Simulink software were studied.

SIMULATION DIAGRAM:

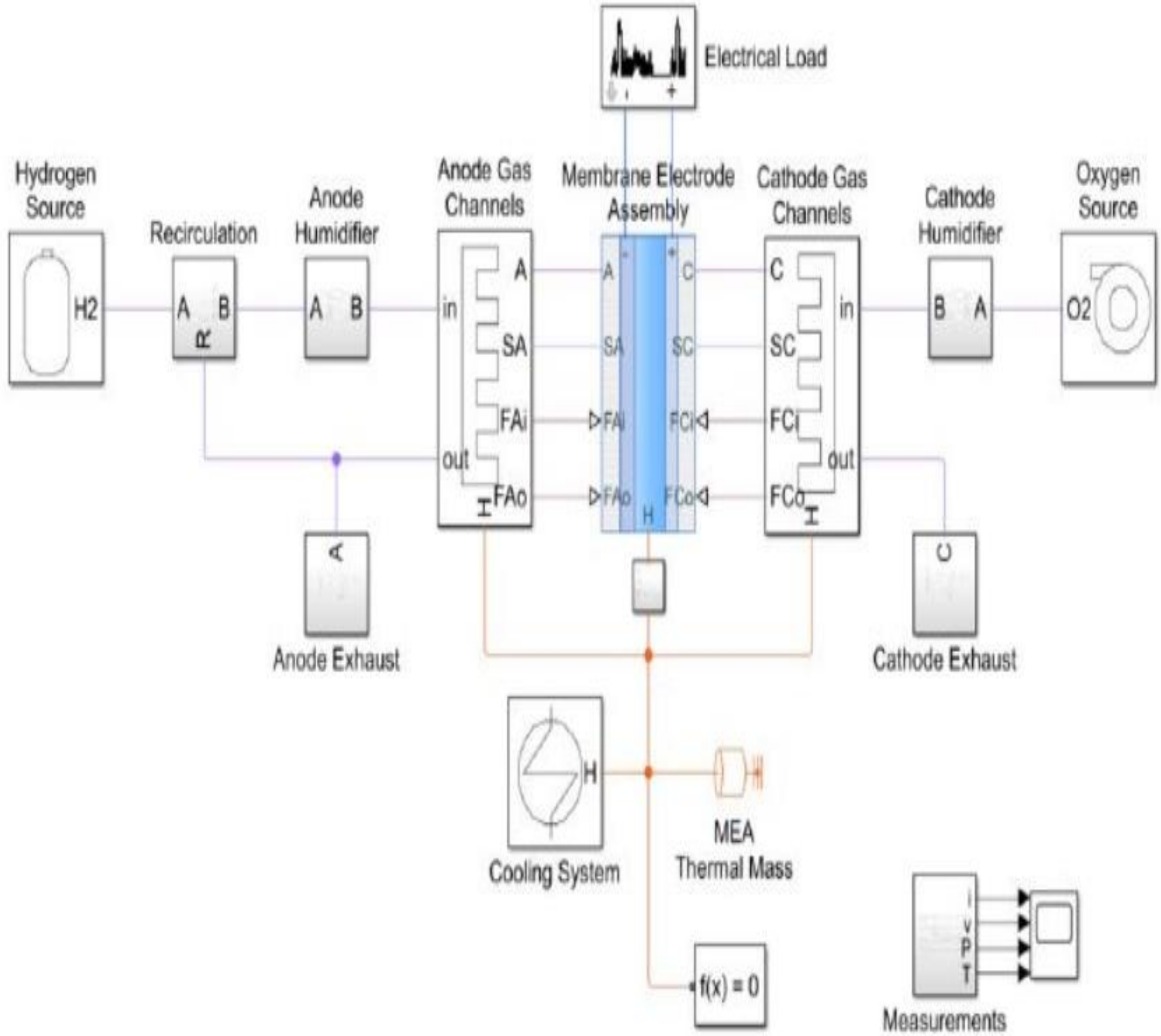

EXP.NO: 3

V-I Characteristics of fuel cell

DATE:

AIM:

To determine the voltage-current characteristics of Fuel Cell.

PROCEDURE:

Set up

- Connect the AC power pack cable to the **12V**DC power input on the FC50 Fuel Cell. Connect the other end of the AC power pack to a source of AC power. On the front panel of the EL200 Electronic Load ensure the toggle switch is **OFF**. Use the AC power cord to connect the EL200 to a source of AC power; then turn on the main power switch located behind the EL200 front panel.
- Use two short test leads to connect the FC50 with the EL200, paying attention to the polarity.
- Attach the hydrogen supply quick-coupler to the FC50. Connect the 9-pin plug of the hydrogen
- supply’s solenoid valve to the **H2 SUPPLY** connector on the FC50.
- Connect the required RS-232 interface to the computer.

Start up

Starting the electrolyser

- Connect the AC power Cable to the supply and switch it ON.
- There will be a self check of 20 seconds by the electrolyser system. After that the main screen of the Graphic display will show STANDBY.
- Press the Start button and wait until the internal pressure reaches 100%. Now the display shows ready.
- Press Open**.** The external pressure will reach to the set pressure and the display will show Normal flow and Normal pressure.
- For the EL200 ensure that the 10-turn potentiometer is set to zero. Then turn ON the toggle switch on the front panel**.**
- Ensure the fan control knob is at **AUTO**. Set the main switch to **ON** and press the **START** button in the FC 50 module. After completing a system test, the green **OPERATION** light comes on and the
- FC50 is ready for use. If an error occurs, the error code will appear in the**H2 Flow** display.

Data acquisition

- For these measurements, the fuel cell should be at a temperature of 35 °C. This temperature can
- be reached by loading the fuel cell for a few minutes with a current of approximately 5 A. Using the potentiometer of the EL200, increase the load current until the Current display on the FC50 shows approximately 5 amperes. To further cause stack temperature to rise, turn the fan control knob on the FC50 so the Fan Power display indicates 10%.After the temperature reaches 35 °C, ensure the load potentiometer is turned back to zero and set fan control knob to AUTO.
- Using the EL200 potentiometer, set in turn each load current listed in theTable1. After waiting at
- least 15 seconds at each point, record the measured values of stack current I stack and stack voltage V stack in the table. When measuring the first point (no-load operation) turn the toggle switch on the EL200 to OFF to ensure that there is no load on the fuel cell.

Shut down procedure

- On the EL200, turn the potentiometer to zero, set the toggle switch to **OFF,** and turnoff the
- main power switch behind the front panel.
- On the FC50, turn the fan control knob to **AUTO** and turn the main switch **OFF**.
- Shut down of the Electrolyser :
  1. Press the close button to cut the hydrogen supply. The display then shows ready mode.
  2. Now press the Stop button so that the electrolyser comes in Standby mode.
  3. Switch off the power supply.

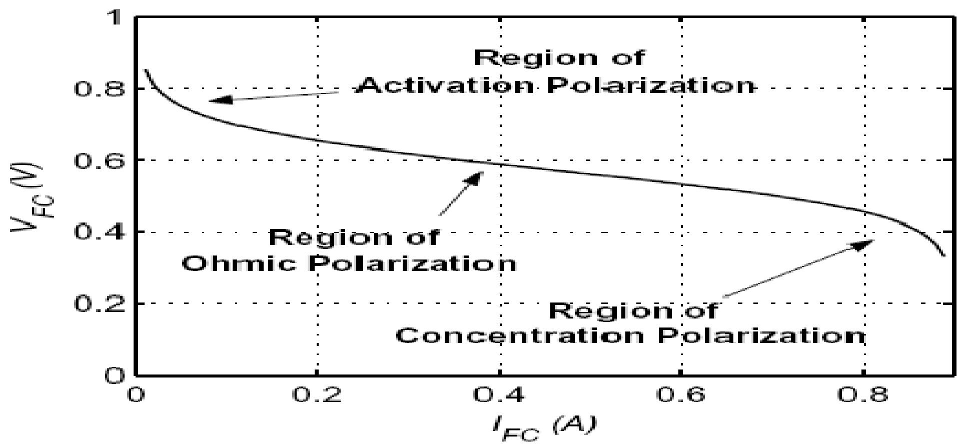

RESULT:

Thus voltage and current parameters fuel cell was determined and verified.

SIMULATION DIAGRAM:

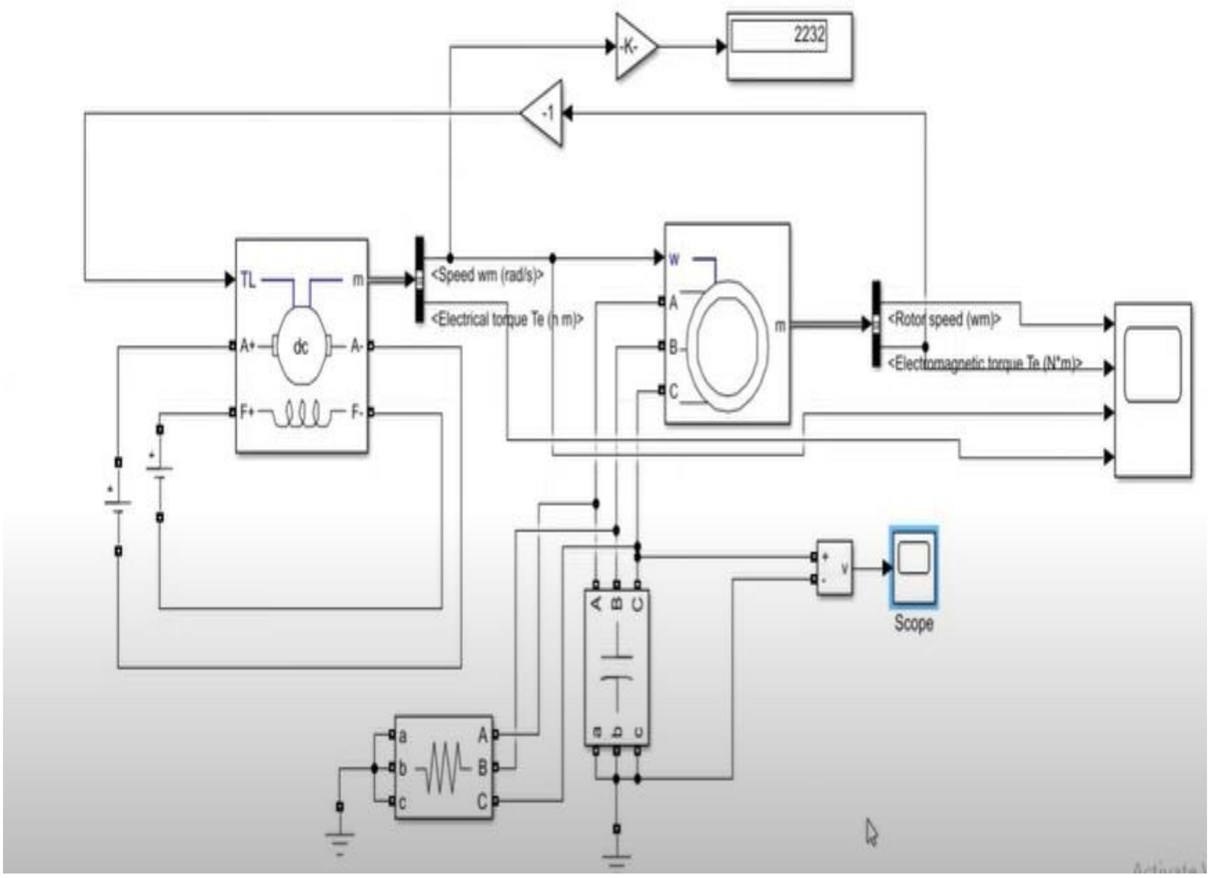

EXP.NO:4 **Performance Characteristics of self – excited Induction Generator**
DATE:

AIM:

To conduct the Simulation and study on Performance Characteristics of self – excited Induction Generator.

THEORY:

Wind turbines work on a simple principle: instead of using electricity to make wind—like a fan wind turbines use wind to make electricity. Wind turns the propeller-like blades of a turbine around a rotor, which spins a generator, which creates electricity.

Wind is a form of solar energy caused by a combination of three concurrent events: The sun unevenly heating the atmosphere, Irregularities of the earth's surface and the rotation of the earthThe terms "wind energy" and "wind power" both describe the process by which the wind is used to generate mechanical power or electricity. This mechanical power can be used for specific tasks (such as grinding grain or pumping water) or a generator can convert this mechanical power into electricity. A wind turbine turns wind energy into electricity using the aerodynamic force from the rotor blades, which work like an airplane wing or helicopter rotor blade. When wind flows across the blade, the air pressure on one side of the blade decreases. The difference in air pressure across the two sides of the blade creates both lift and drag. The force of the lift is stronger than the drag and this causes the rotor to spin. The rotor connects to the generator, either directly (if it's a direct drive turbine) or through a shaft and a series of gears (a gearbox) that speed up the rotation and allow for a physically smaller generator. This translation of aerodynamic force to rotation of a generator creates electricity.

FORMULA:

Power (W) = 0.6 x Cp x N x A x V3 .

Revolutions (rpm) = V x TSR x 60 / (6.28 x R),

Where

Cp = Rotor efficiency,

N = Efficiency of driven machinery,

A = Swept rotor area (m2),

V = Wind speed (m/s)

TSR = Tip Speed Ratio,

R = Radius of rotor, Rotor efficiency can go as high as Cp = 0.48, but Cp = 0.4

Regenerate Initial Conditions

This example is set-up with all states initialized so that the simulation starts in steady-state. Otherwise, due to the long time constants of the electromechanical part of the wind turbine model and to its relatively slow regulators you would have to wait for tens of seconds before reaching steady-state. The initial conditions have been saved in the "power_wind_dfig_det.mat" file. When you start simulation, the InitFcn callback (in the Model Properties/Callbacks) automatically loads into your workspace the contents of this .mat file ("xInitial" variable specified in the "Initial state" parameter in the Simulation/Configuration Parameters menu).

If you modify this model, or change parameter values of power components, the initial conditions stored in the "xInitial" variable will no longer be valid and Simulink® will issue an error message. To regenerate the initial conditions for your modified model, follow the steps listed below:

1. In the Simulation/Configuration Parameters menu, uncheck the "Initial state" parameter.

2. In the 120 kV Three-phase Voltage Source menu, disable the source voltage step by setting the "Time variation of" parameter to "none".

3. In order to shorten the time required to reach steady-state, you will have to temporarily decrease the inertia of the turbine-generator group. Open the DFIG Wind Turbine menu and in the Drive train data and Generator data, divide the H inertia constants by 10.

4. Change the Simulation Stop Time to 5 seconds. Note that in order to generate initial conditions coherent with the 60 Hz voltage source phase angles, the Stop Time must be an integer number of 60 Hz cycles.

5. Change the Simulation Mode from "Normal" to "Accelerator".

6. Start simulation. When Simulation is completed, verify that steady state has been reached by looking at waveforms displayed on the Scope block. The final states which have been saved in the "xFinal" structure with time can be used as initial states for future simulations. Executing the next two commands copies these final conditions in "xInitial" and saves this variable in a new file (myModel_init.mat). * >> xInitial=xFinal; * >> save myModel_init xInitial

7. In the File/Model Properties/Callbacks/InitFcn window, replace the first line of initialization commands with "load myModel_init". Next time you start a simulation with this model, the variable xInitial saved in the myModel_init.mat file will be loaded in your workspace.

8. In the Simulation/Configuration Parameters menu, check "Initial state".

9. In the Wind Turbine Generator and Drive train data, reset the inertia constants H back to their original values.

10. Start simulation and verify that your model starts in steady-state.

11. In the 120 kV Three-phase voltage source menu, set the "Time variation of" parameter back to "Amplitude".

12. Change the Simulation Stop Time and Simulation Mode back to their original values (0.2 seconds, Normal).

13. Save your Model.

WIND TURBINE INPUT:

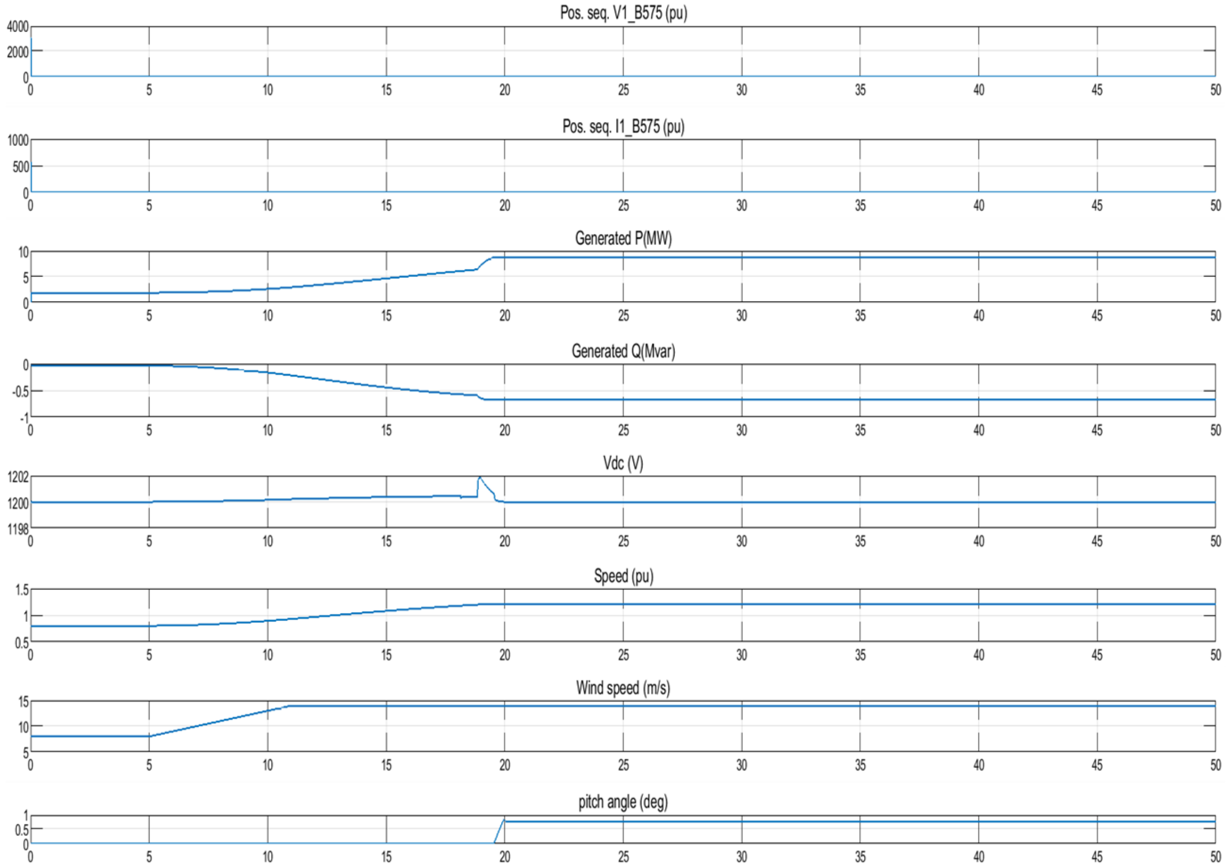

Grid Output

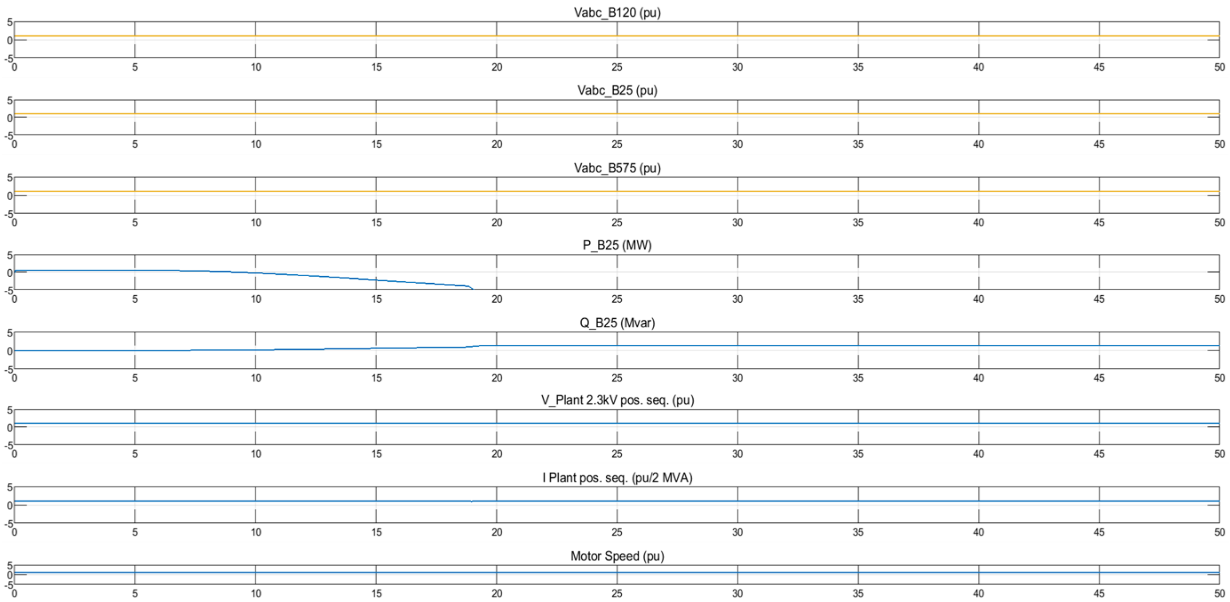

RESULT:

The Simulation on Performance Characteristics of self – excited Induction were studied.

SIMULATION DIAGRAM:

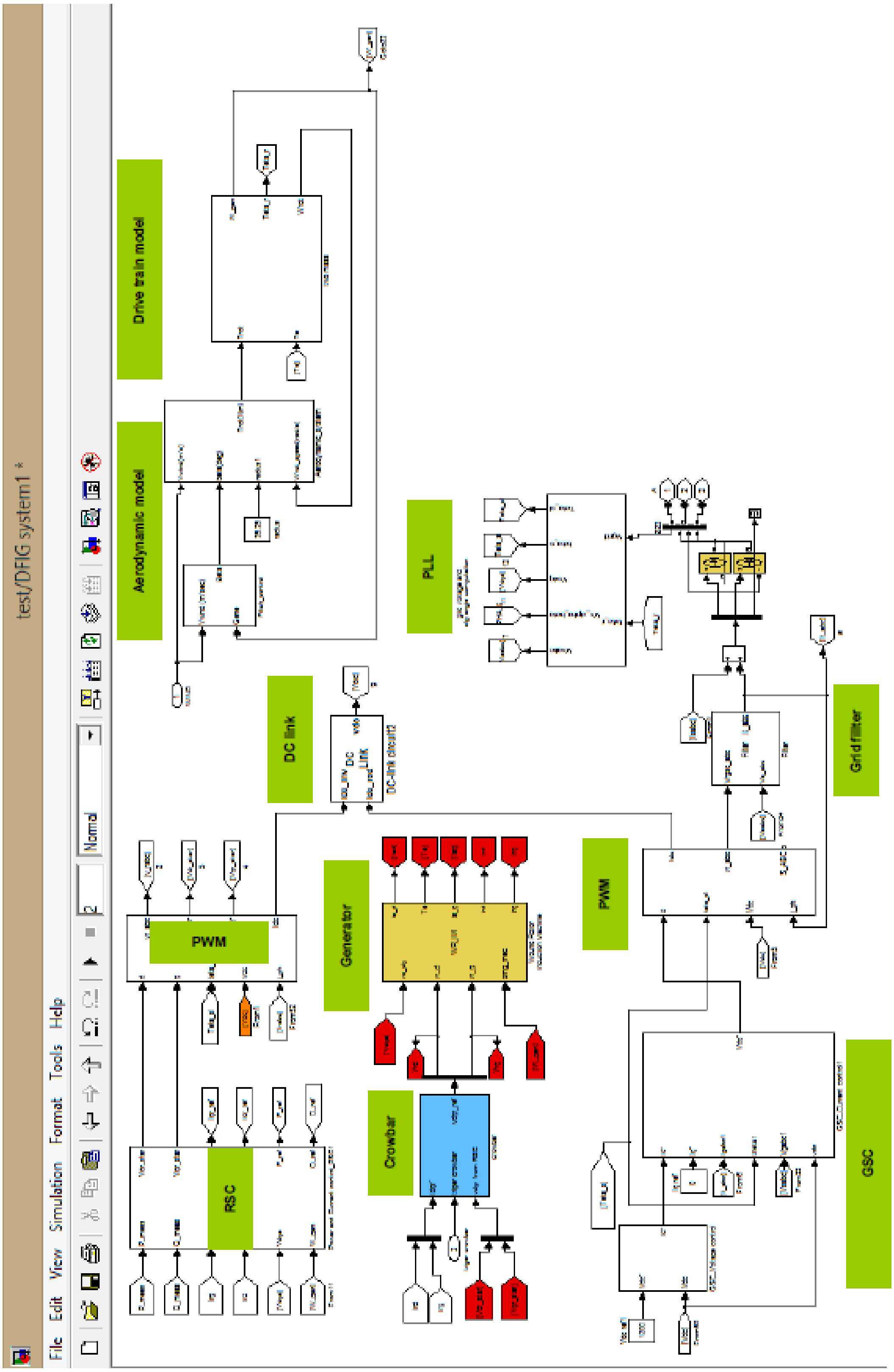

EXP.NO : 5

Performance Characteristics of DFIG

DATE:

AIM:

To study Performance Characteristics of DFIG using MATLAB /simulink .

THEORY:

The equivalent circuit of a DFIG shown in figure 3.1 can be characterized by different reference frames such as the stationary frame, rotor frame, or the synchronous frame oriented to either stator flux or stator voltage. The simplified DFIG model can be described as three windings in the stator and three windings in the rotor, as shown in figure. The System configuration of the DFIG-based wind turbine

$$v_{as}(t) = r_s i_{as}(t) + \rho\lambda_{as}(t)$$

$$v_{bs}(t) = r_s i_{bs}(t) + \rho\lambda_{bs}(t)$$

$$v_{cs}(t) = r_s i_{cs}(t) + \rho\lambda_{cs}(t)$$

$$v_{ar}(t) = r_r i_{ar}(t) + \rho\lambda_{ar}(t)$$

$$v_{br}(t) = r_r i_{br}(t) + \rho\lambda_{br}(t)$$

$$v_{cr}(t) = r_r i_{cr}(t) + \rho\lambda_{cr}(t)$$

where:-

r_s: is the stator resistance.

r_r : is the rotor resistance referred to the stator.

$v_{as}(t)$,$v_{bs}(t)$, and $v_{cs}(t)$: are the applied stator voltages.

$i_{as}(t)$,$i_{bs}(t)$, and $i_{cs}(t)$: are the stator currents of phases.

$v_{ar}(t)$,$v_{br}(t)$, and $v_{cr}(t)$: are the stator referred rotor voltages.

$i_{ar}(t)$,$i_{br}(t)$, and $i_{cr}(t)$: are the stator referred rotor currents of phases.

$\lambda_{as}(t)$,$\lambda_{bs}(t)$, and $\lambda_{cs}(t)$: are the stator fluxes.

$\lambda_{ar}(t)$,$\lambda_{br}(t)$, and $\lambda_{cr}(t)$: are the rotor fluxes.

At steady state condition the following hold:-

- The stator side electric magnitudes have a constant sinusoidal angular frequency (ω_e).

The rotor side electric magnitudes have a constant angular frequency .

BLOCK DIAGRAM:

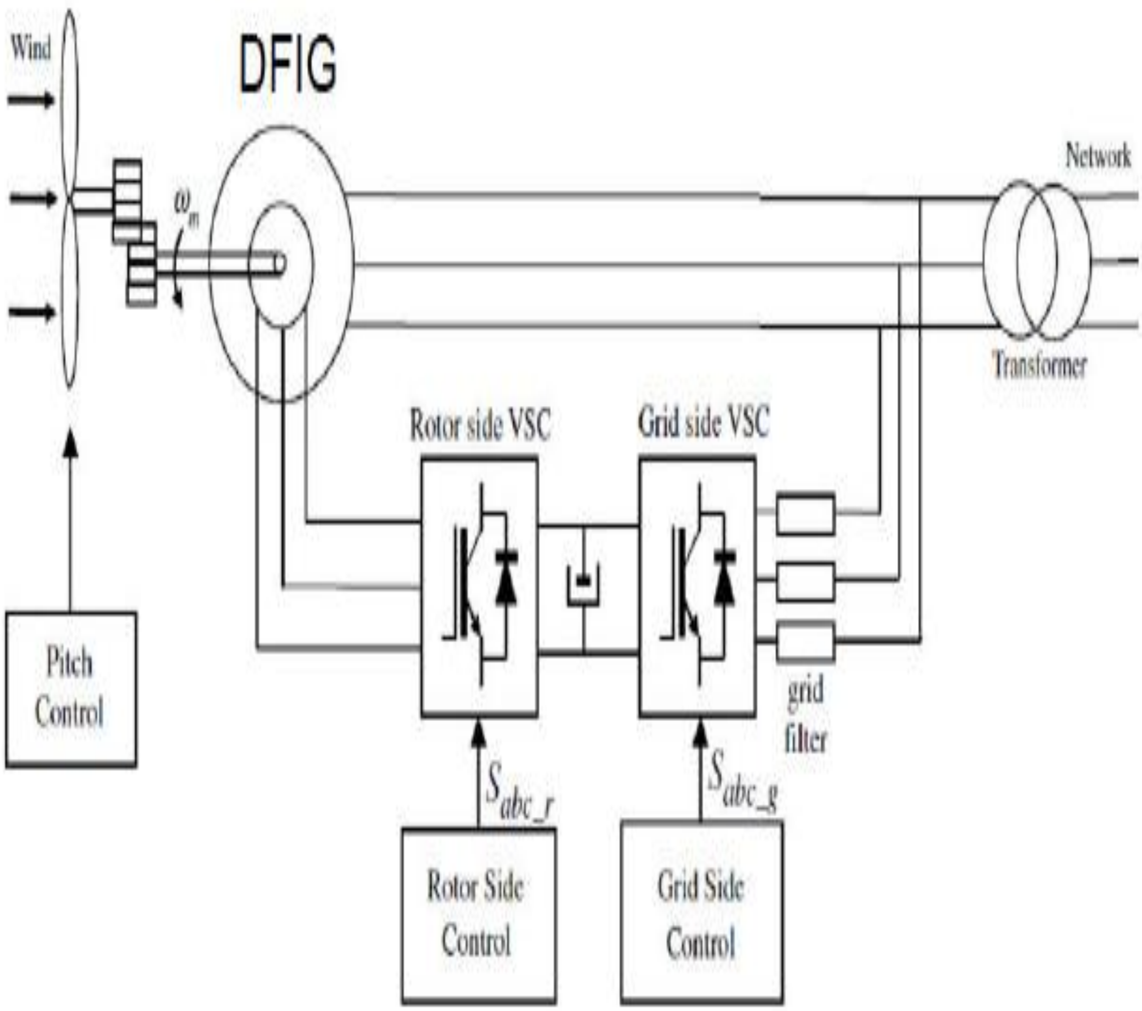

The relationship between the stator angular frequency and the rotor angular frequency

can be expressed as:

$$\omega_r + \omega_m = \omega_e$$

where (ω_m) is the electrical angular frequency of the machine.

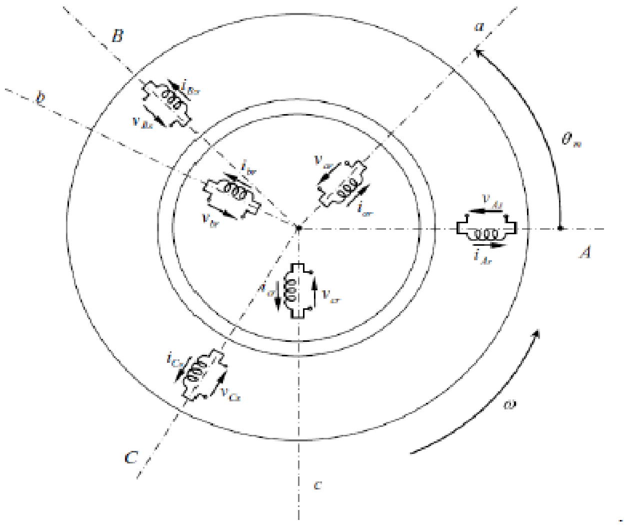

Ideal three-phase windings (stator and rotor) of the DFIG

In generalized electrical machine theory, the inclusion of space vector analysis is based on the following hypotheses shown in:

1. The distributions of flux and magneto-motive force (MMF) are represented by their fundamental harmonic component alone.

2. The effect of slotting winding distribution can be neglected.

3. Commutation effects and brush-connections are considered to be ideal.

4. The influences of eddy currents and hysteresis can be neglected.

5. Magnetic saturation is not present.

Magnetic linearity is assumed in order to produce linear superimposition magnetic fields, which simplifies model development considerably. In practical, if magnetic saturation has an effect on the machine, it will limit the transient over-shoot current and power in the step response of the vector control, and restrict the instant excesses of fault response. The linear magnetic analysis will therefore derive a worst-case response in terms of transient response to both control and faults. Therefore, the stator and rotor voltage and magnetic flux equations of the DFIG in the stationary reference ($\alpha\beta$) frame are as follows,

$$v_{\alpha s} = r_s i_{\alpha s} + \rho\lambda_{\alpha s}$$

$$v_{\beta s} = r_s i_{\beta s} + \rho\lambda_{\beta s}$$

$$v_{\alpha r} = r_r i_{\alpha r} + \omega_r \lambda_{\beta r} + \rho\lambda_{\alpha r}$$

$$v_{\beta r} = r_r i_{\beta r} - \omega_r \lambda_{\alpha r} + \rho\lambda_{\beta r}$$

In the (dq) frame, the voltages can describe as:

$$v_{qs} = r_s i_{qs} + \omega_e \lambda_{ds} + \rho\lambda_{qs}$$

$$v_{ds} = r_s i_{ds} - \omega_e \lambda_{qs} + \rho\lambda_{ds}$$

$$v_{qr} = r_r i_{qr} + (\omega_e - \omega_r)\lambda_{dr} + \rho\lambda_{qr}$$

$$v_{dr} = r_r i_{dr} - (\omega_e - \omega_r)\lambda_{qr} + \rho\lambda_{dr}$$

where: $\rho = d/dt$, and the stator and rotor flux linkage equations in the $(\alpha\beta)$ frame are:

$$\lambda_{\alpha s} = L_s i_{\alpha s} + L_m i_{\alpha r} e^{j\theta_r}$$

$$\lambda_{\beta s} = L_s i_{\beta s} + L_m i_{\beta r} e^{j\theta_r}$$

$$\lambda_{\alpha r} = L_m i_{\alpha s} + L_r i_{\alpha r} e^{j\theta_r}$$

$$\lambda_{\beta r} = L_m i_{\beta s} + L_r i_{\beta r} e^{j\theta_r}$$

The stator and rotor flux linkage equations in the (dq) frame are:-

$$\lambda_{qs} = L_s i_{qs} + L_m i_{qr}$$

$$\lambda_{ds} = L_s i_{ds} + L_m i_{dr}$$

$$\lambda_{qr} = L_m i_{qs} + L_r i_{qr}$$

$$\lambda_{dr} = L_m i_{ds} + L_r i_{dr}$$

The stator and rotor active and reactive power in the ($\alpha\beta$) frame are calculated as follows:

$$P_s = \frac{3}{2} Re\{\overline{v_s}.\overline{i_s^*}\} = \frac{3}{2}(v_{\alpha s}i_{\alpha s} + v_{\beta s}i_{\beta s})$$

$$P_r = \frac{3}{2} Re\{\overline{v_r}.\overline{i_r^*}\} = \frac{3}{2}(v_{\alpha r}i_{\alpha r} + v_{\beta r}i_{\beta r})$$

$$Q_s = \frac{3}{2} Im\{\overline{v_s}.\overline{i_s^*}\} = \frac{3}{2}(v_{\beta s}i_{\alpha s} - v_{\alpha s}i_{\beta s})$$

$$Q_r = \frac{3}{2} Im\{\overline{v_r}.\overline{i_r^*}\} = \frac{3}{2}(v_{\beta r}i_{\alpha r} - v_{\alpha r}i_{\beta r})$$

The stator/rotor active and reactive power and electromagnetic torque expressions in (dq) frame:-

$$P_s = \frac{3}{2} Re\{\overline{v_s}.\overline{i_s^*}\} = \frac{3}{2}(v_{ds}i_{ds} + v_{qs}i_{qs})$$

$$Q_s = \frac{3}{2} Im\{\overline{v_s}.\overline{i_s^*}\} = \frac{3}{2}(v_{qs}i_{ds} - v_{ds}i_{qs})$$

$$P_r = \frac{3}{2} Re\{\overline{v_r}.\overline{i_r^*}\} = \frac{3}{2}(v_{dr}i_{dr} + v_{qr}i_{qr})$$

$$Q_r = \frac{3}{2} Im\{\overline{v_r}.\overline{i_r^*}\} = (v_{qr}i_{dr} - v_{dr}i_{qr})$$

where the superscript * represents the complex conjugate of a space vector, as used in phasors. Finally, the electromagnetic torque can be found from:

$$T_e = \frac{3}{2} Im\{\overline{\lambda_s}.\overline{i_r^*}\} = \frac{3}{2} p \frac{L_m}{L_s}(\lambda_{qs}i_{dr} - \lambda_{ds}i_{qr})$$

Drive Train Model :

The drive train system could be approximated by a two-mass mechanical spring and damper model connected by a flexible shaft characterized by stiffness and damping coefficients that modeled on the low speed shaft, while the high speed shaft is assumed to be stiff. This gives more accurate responses of the wind turbines during fluctuating wind conditions. This dynamical model is widely accepted as expressing the dynamical behaviour of the drive train in this area of research. The inertia of the low speed shaft comes mainly from the rotating blades and the inertia of the high speed shaft from the generator. The mass of the gearbox itself is insignificant and neglected. Stiffness and damping of the shaft are combined in one equivalent for stiffness and damping placed at the low speed side The aerodynamic torque T_w and the generator reaction torque T_e represent the input quantities for the model while changes in turbine‘s rotor speed and generator speed are the output. The variation in the angular generator speed and angular rotor speed respectively expressed as

$$T_m - T_e = J_{gen}\frac{d\omega_{gen}}{dt}$$

$$T_w - T_{shaft} = J_{rot}\frac{d\omega_{rot}}{dt}$$

where:

$$T_m = \frac{T_{shaft}}{K_{gear}}, \quad \text{and} \quad T_{shaft} = K_{shaft}\,\Delta\theta + D_{shaft}\,\Delta\omega$$

$$\frac{d\theta_{rot}}{dt} = \omega_{rot}$$

$$\frac{d\theta_{gen}}{dt} = \omega_{gen}$$

Therefore, after substitution the above equations are simplified to derive the torque equations given by the following:

$$T_w = J_{rot}\frac{d\omega_{rot}}{dt} + K_{shaft}\left(\theta_{rot} - \frac{\theta_{gen}}{K_{gear}}\right) + D_{shaft}\left(\omega_{rot} - \frac{\omega_{gen}}{K_{gear}}\right)$$

$$-T_e = J_{gen}\frac{d\omega_{gen}}{dt} - \frac{K_{shaft}}{K_{gear}}\left(\theta_{rot} - \frac{\theta_{gen}}{K_{gear}}\right) - \frac{D_{shaft}}{K_{gear}}\left(\omega_{rot} - \frac{\omega_{gen}}{K_{gear}}\right)$$

$$\frac{d\omega_{rot}}{dt} = \frac{1}{J_{rot}}\left(T_w - K_{shaft}\left(\theta_{rot} - \frac{\theta_{gen}}{K_{gear}}\right) - D_{shaft}\left(\omega_{rot} - \frac{\omega_{gen}}{K_{gear}}\right)\right)$$

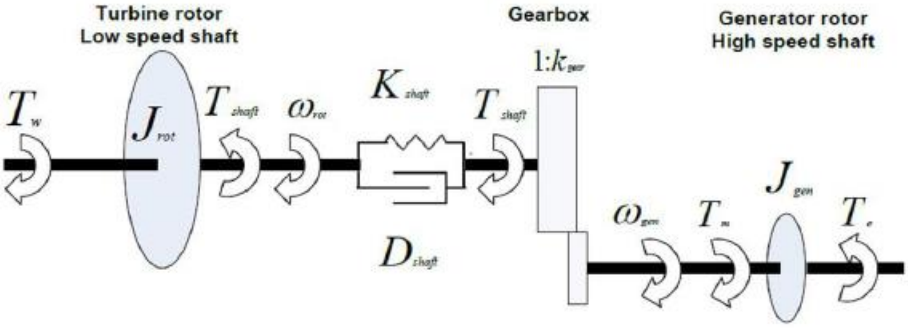

$$\frac{d\omega_{gen}}{dt} = \frac{1}{J_{gen}}\left(-T_e + K_{shaft}\left(\theta_{rot} - \frac{\theta_{gen}}{K_{gear}}\right) + D_{shaft}\left(\omega_{rot} - \frac{\omega_{gen}}{K_{gear}}\right)\right)$$

Two-mass-model for the drive train

Wind Turbine Power Characteristics:

The wind turbines convert aerodynamic power into electrical energy. In a wind turbine, two conversion processes take place. The first converts the aerodynamic power that is available in the wind into mechanical power. The next process converts the mechanical power into electrical power.

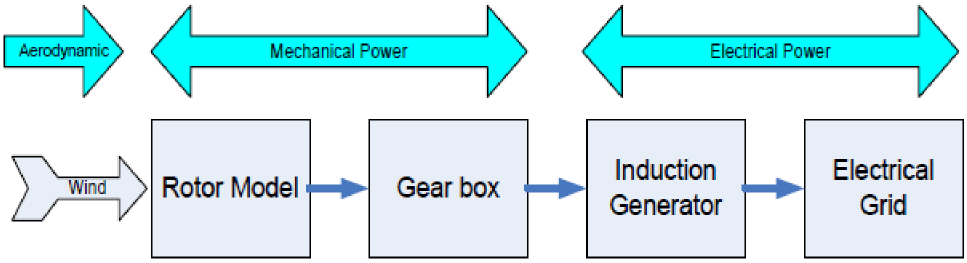

Block diagram of wind energy conversion system.

The DFIG system in the Simulink model includes: the generator, a bidirectional power electronic converter, a digital controller with cascaded feedback control schemes, crowbar, a two-mass drive-shaft model to represent the wind turbine mechanical dynamics, a simplified wind turbine controller and a simplified network model. The wind turbine in this study is on 1.5MW, with a horizontal axis, and three-bladed with blad radius 35.25 m, upwind wind turbine with pitch control. A two-pair pole DFIG using back-to-back PWM voltage source converters in the rotor winding circuit, is adopted in the wind turbine with carrier frequency of 5 KHz and average voltage 398.74 V, and 0.9 is the value of the setting factor which calculated from the equation $\left(\text{setting factor} = \frac{Nominal\ voltage\ value \times \sqrt{2}}{Average\ voltage\ vlaue}\right)$.

The parameters used in the DFIG based wind turbine model are close to that of a commercial wind turbine as illustrated in appendix A. The rotor-circuit crowbar model is connected by the rotor winding of the DFIG. When activated, the DFIG rotor voltage was rendered zero, since its short circuit the rotor winding to isolate the RSC. When disengaged, the crowbar had no effect on the rotor circuit and the RSC voltage was passed unchanged to the rotor of the DFIG. In the simulation assume an infinitely stiff grid is assumed which entails an ideal voltage source. Specific voltage dips or swells can be applied to the DFIG system with specific period time during system operation. The modelled voltages were applied directly to the stator connection of the DFIG model.

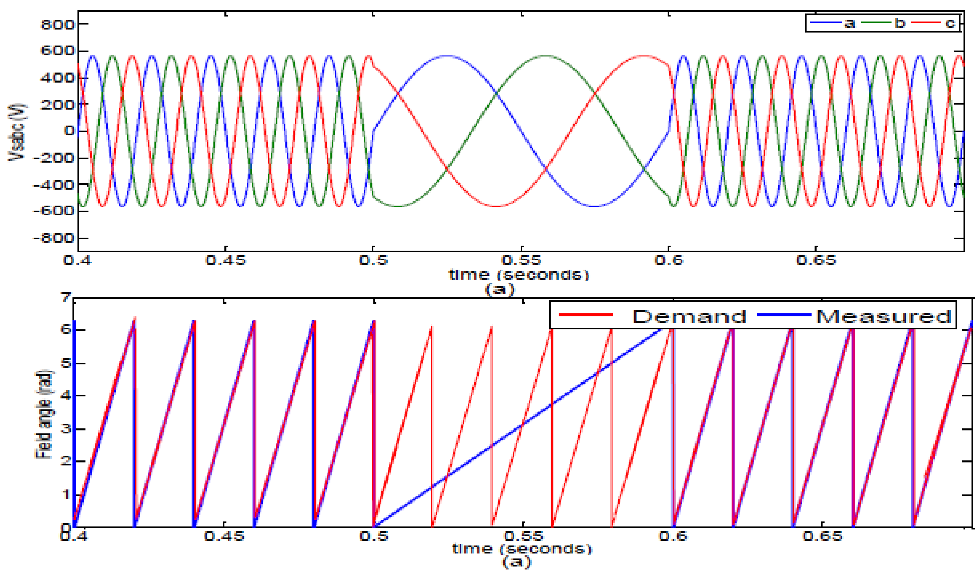

Instantaneous measurements of (a) grid voltage and (b) PLL response after 40Hz frequency step change.

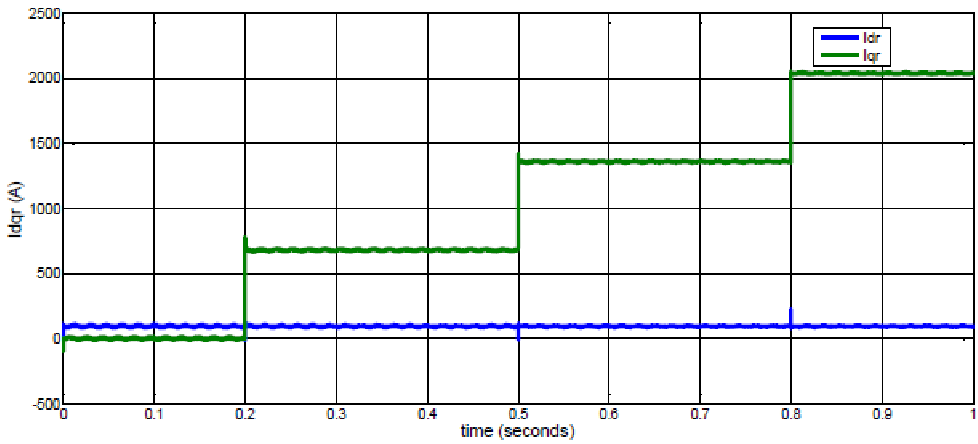

Instantaneous measurements of the rotor current in synchronous reference frame i_{dqr}

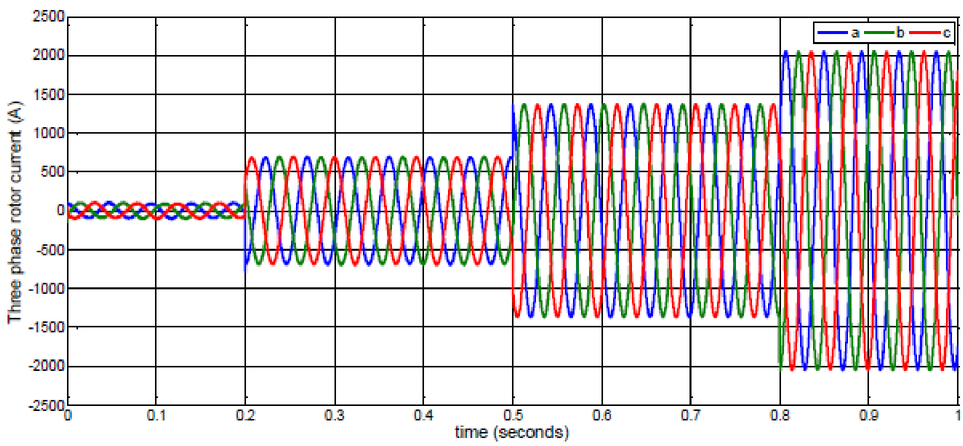

Instantaneous measurements of the three phase rotor current.

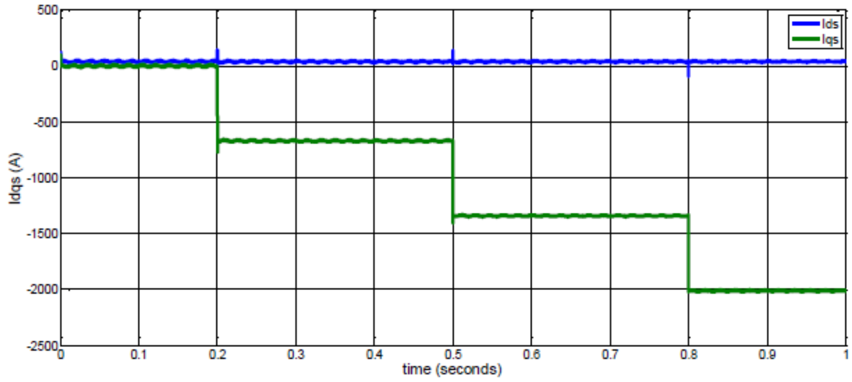

Instantaneous measurements of the stator current in synchronous reference frame i_{dqs}

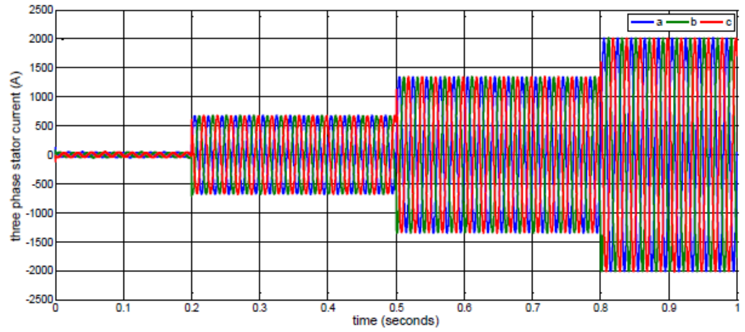

Figure 3.39: Instantaneous measurements of the three-phase stator current.

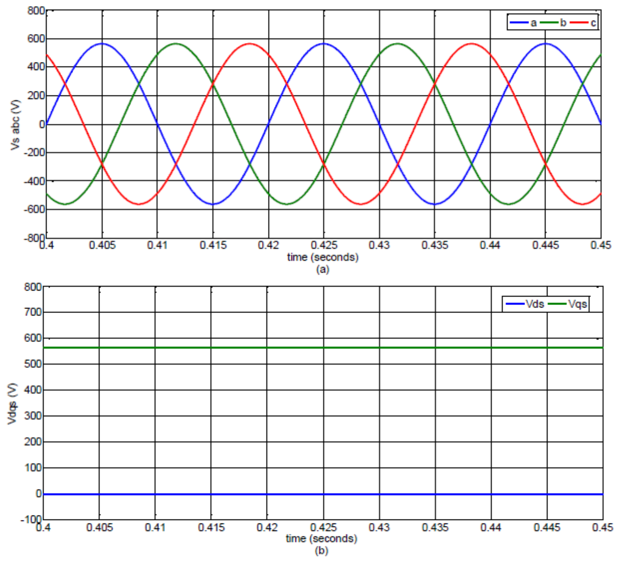

Figure 3.40: Instantaneous measurements of the grid voltage: (a) three phase; (b) in synchronous reference frame coordination.

RESULT:

Thus the Performance Characteristics of DFIG using MATLAB /simulink were studied.

EX.NO: 6 Performance Characteristics of PMSG

DATE:

AIM:

To study the Performance Characteristics of PMSG using MATLAB / Simulink.

THEORY:

Permanent Magnet Synchronous Generator (PMSG), which is based on variable-speed operation, has been used . Since the speed of wind turbine is variable, the generator is controlled by power electronic devices. A rectifier is used to rectify the output voltage of PMSG and DC/DC buck converter is used to decrease this rectified voltage to that of battery and connected DC load. permanent magnet synchronous generator (PMSG) offers better performance due to higher efficiency and less maintenance because it does not have rotor current. PMSG can be used without a gearbox, which implies a reduction of the weight of the nacelle and reduction of costs

PMSG Driven System:

The direct driven wind turbine concept with multi-pole permanent magnet synchronous generator (PMSG) and full-scale frequency converter is a promising but not yet very popular wind turbine concept for modern wind turbines. The gearless PMSG with full-scale converter. As a gearbox causes greater weight, losses, costs and demands maintenance, a gearless structure represents an efficient and robust answer, which could be very favorable especially for offshore applications. Moreover, due to the permanent magnet excitation of the generator the DC excitation system can be eliminated, decreasing again weight, losses, costs and maintenance requirements. The efficiency of a PMSG wind turbine is thus assessed to be higher than for other concepts. However, the disadvantages of the permanent magnet excitation are the still high costs for permanent magnet materials and a fixed excitation, which cannot be varied according to the working condition requirement. As multi-pole permanent magnet generators are low speed applications and generally connected to the grid using a frequency converter system, the generator has no damper winding in the rotor core. Moreover, due to the permanent excitation a PMSG has no field windings, in which transient currents could be induced or damped respectively. Hence, in case of load changes the field windings would not contribute to damping either. As neither a damper nor field winding exists in a PMSG, no transient or sub-transient reactance can be defined for the PMSG.

i.e.

$X_d = X_d' = X_d''$

$X_q = X_q' = X_q''$

where

X_d and X_q -synchronous reactance

X_d' and X_q' -transient reactance

X_d'' and X_q'' -sub-transient reactance

SIMULATION DIAGRAM

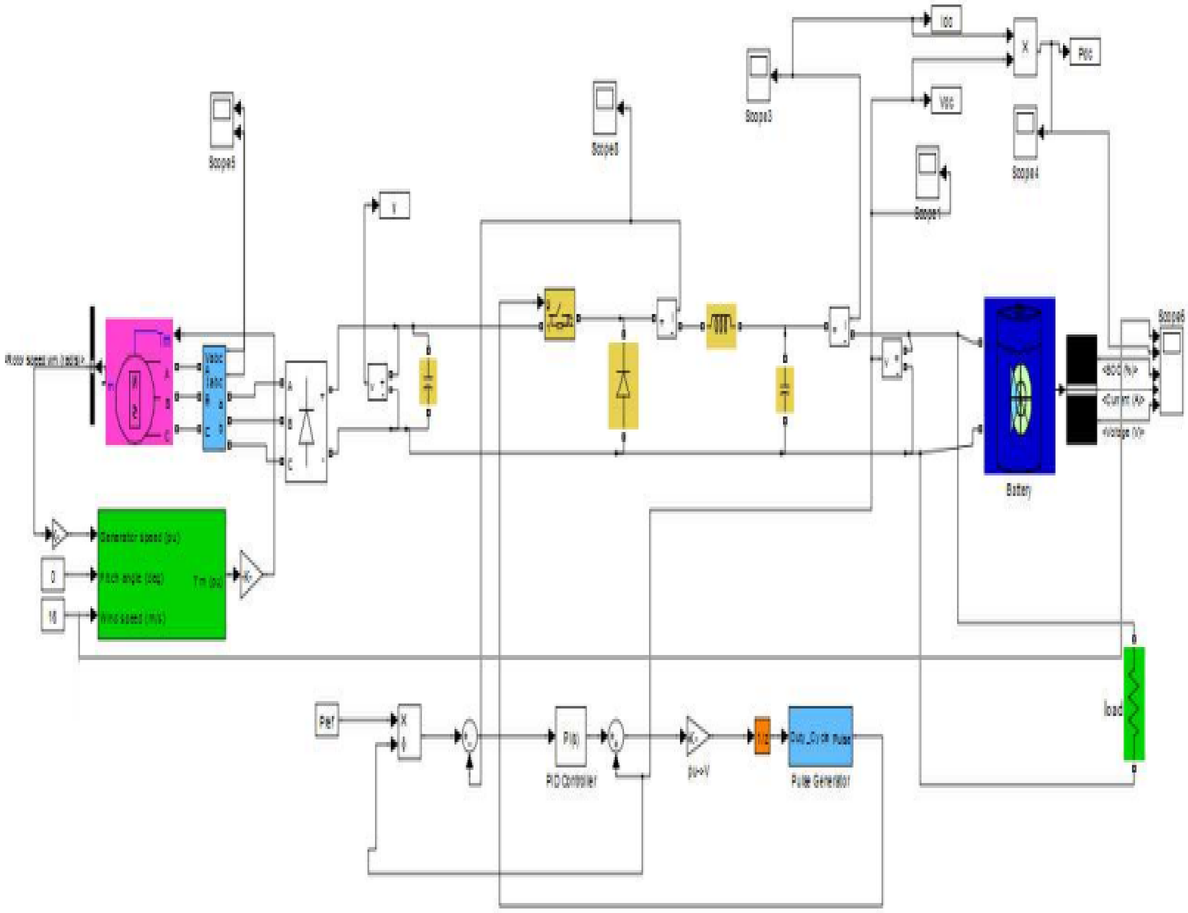

Simulation model of standalone wind system

OUTPUT WAVEFORM:

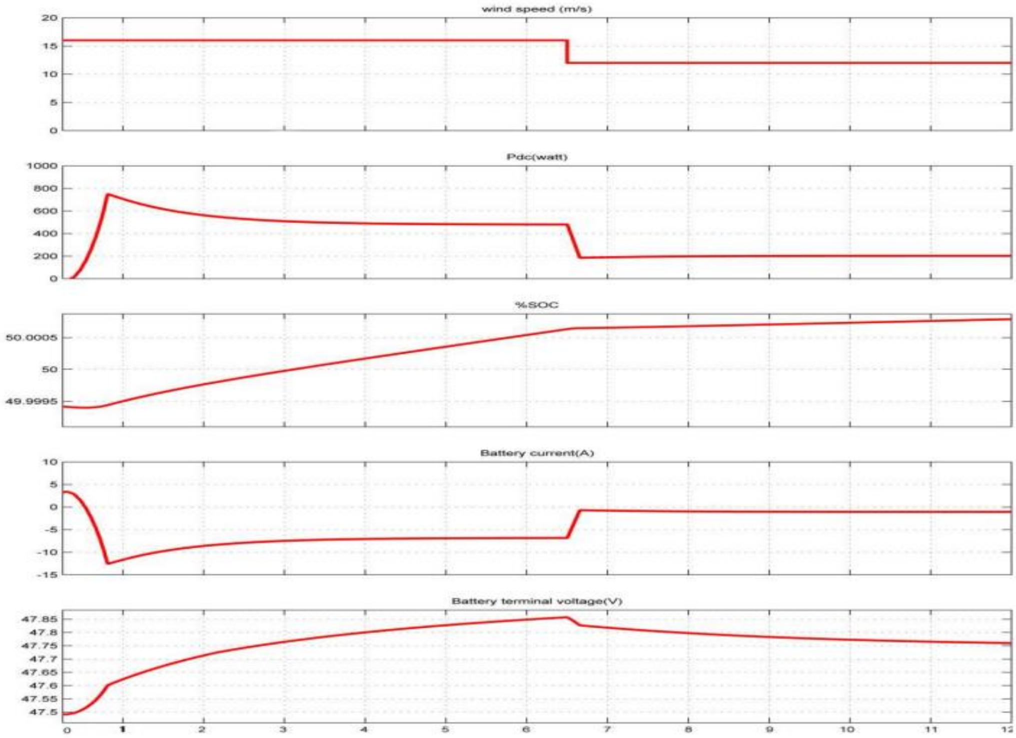

Figure 10. Different characteristics of the simulated wind system for step change in wind speed from 16m/s to 12m/s

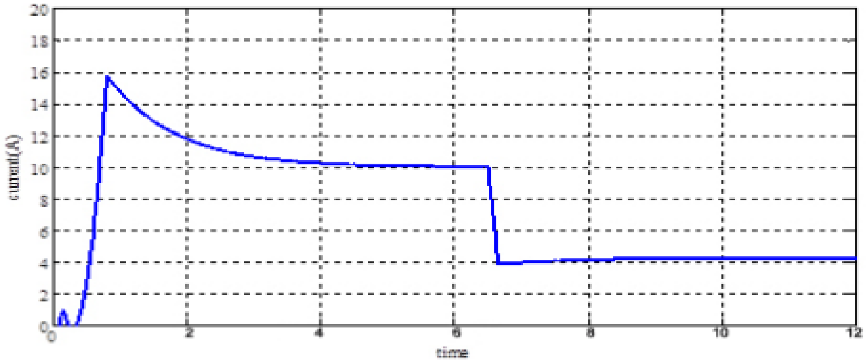

Figure 11. Output current

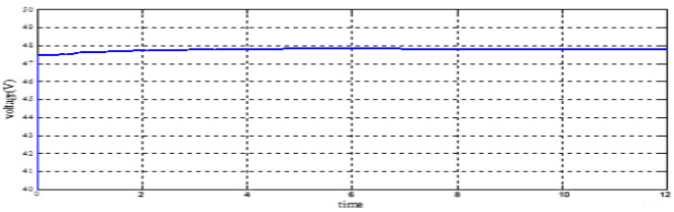

Figure 12. Output Voltage

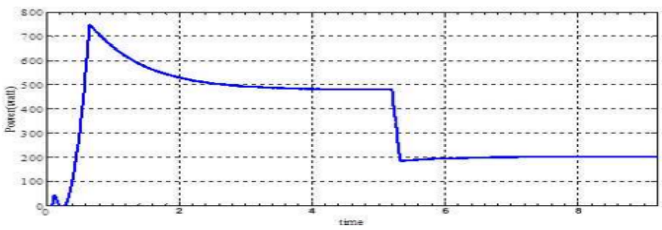

Figure 13. Output power (Pdc) across battery and load

RESULT:

Thus the Performance Characteristics of PMSG using MATLAB / Simulink were studied.

SIMULATION:

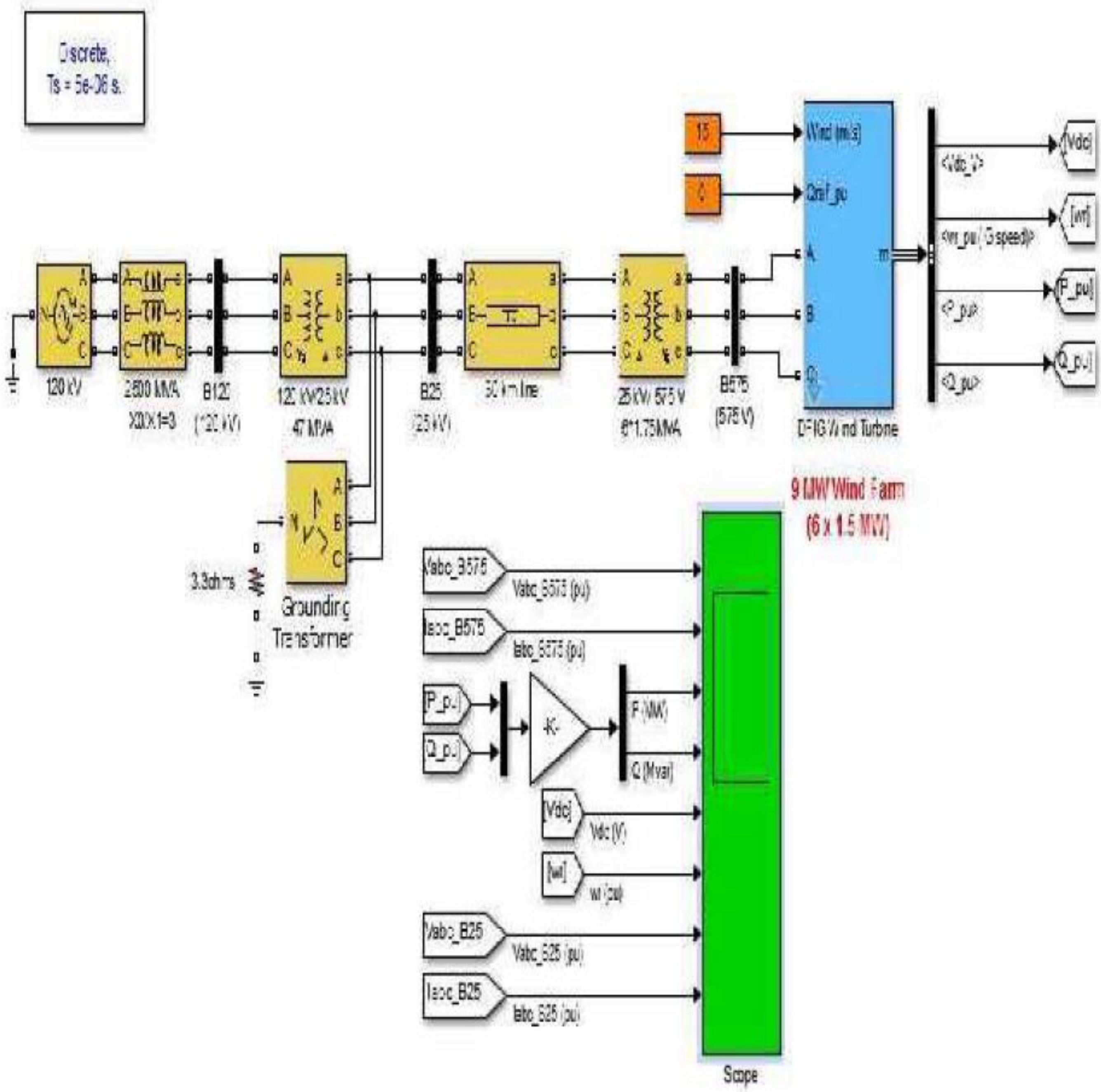

Wind Farm - DFIG Detailed Model

EXP.NO:7 **MPPT tracking of DFIG based WT**

DATE:

AIM:

To study the MPPT tracking of DFIG based WT.

THEORY:

FUNDAMENTALS OF WIND TURBINES.

The power extracted from the wind can be calculated by the given formula:

$$P_w = 0.5\rho\pi R^2 V^3 C_p(\lambda,\beta)$$

P_w = extracted power from the wind,

ρ = air density, (approximately 1.225 kg/m^3 at 20° C at sea level)

R = blade radius (in m), (it varies between 40-60 m)

V_w = wind velocity (m/s) (velocity can be controlled between 3 to 30 m/s)

C_p = the power coefficient which is a function of both tip speed ratio (λ), and blade pitch angle, (β) (Degrees)

Power coefficient (C_p) is defined as the ratio of the output power produced to the power available in the wind.

Betz Limit:

No wind turbine could convert more than **59.3%** of the kinetic energy of the wind into Mechanical energy turning a rotor. This is known as the Betz Limit, and is the theoretical Maximum coefficient of power for any wind turbine. The maximum value of $\mathbf{C_p}$ according to Betz limit is 59.3%. For good turbines it is in the range of 35-45%.

Wind Turbine Control Systems

Pitch Angle Control:

The system changes the pitch angle of the blades according to the variation of wind speed. As discussed earlier, with pitch control, it is possible to achieve a high efficiency by continuously aligning the blade in the direction of the relative wind.

On a pitch controlled machine, as the wind speed exceeds its rated speed, the blades are gradually turned about the longitudinal axis and out of the wind to increase the pitch angle. This reduces the aerodynamic efficiency of the rotor, and the rotor output power decreases. When the wind speed exceeds the safe limit for the system, the pitch angle is so changed that the power output reduces to zero and the machine shifts to the „stall" mode. After the gust passes, the pitch angle is reset to the normal position and the turbine is restarted. At normal wind speeds, the blade pitch angle should ideally settle to a value at which the output power equals the rated power. The input variable to the pitch controller is the error signal arising from the difference between the output electrical power and the reference power. The pitch controller operates the blade actuator to alter the pitch angle. During operation below the rated speed, the control system endeavours to the pitch the blade at an angle that maximises the rotor efficiency. The generator must be able to absorb the mechanical power output and deliver to the load. Hence, the generator output power needs to be simultaneously adjusted.

StallControl

Passive stall control:

Generally, stall control to limit the power output at high winds is applied to constant-pitch turbines driving induction generators connected to the network. The rotor speed is fixed by the network, allowing only 1-4% variation. As the wind speed increases, the angle of attack also increases for a blade running at a near constant speed. Beyond a particular angle of attack, the lift force decreases, causing the rotor efficiency to drop. This lift force can be further reduced to restrict the power output at high winds by properly shaping the rotor blade profile to create turbulence on the rotor blade side not facing the wind.

MATLAB CODE:

```
%meshgrid(tsr,pitch);
Cp=0;
c1=0.5176;
c2=116;
c3=0.4;
c4=5;
c5=21;
c6=0.0068;
n=size(tsr);
for i=1:6
for j=1:n(2)
tsr_i=(1/(tsr(j)+0.08*pitch(i))-0.035/(pitch(i)^3+1))^(-1);
Cp(j)=c1*(c2/tsr_i-c3*pitch(i)-c4)*exp(-c5/tsr_i)+c6*tsr(j);
end
plot(tsr,Cp);
hold on;
end
axis ([0 15 -0.1 0.5 ]);
xlabel('\lambda'),ylabel('Cp');
```

OUTPUT:

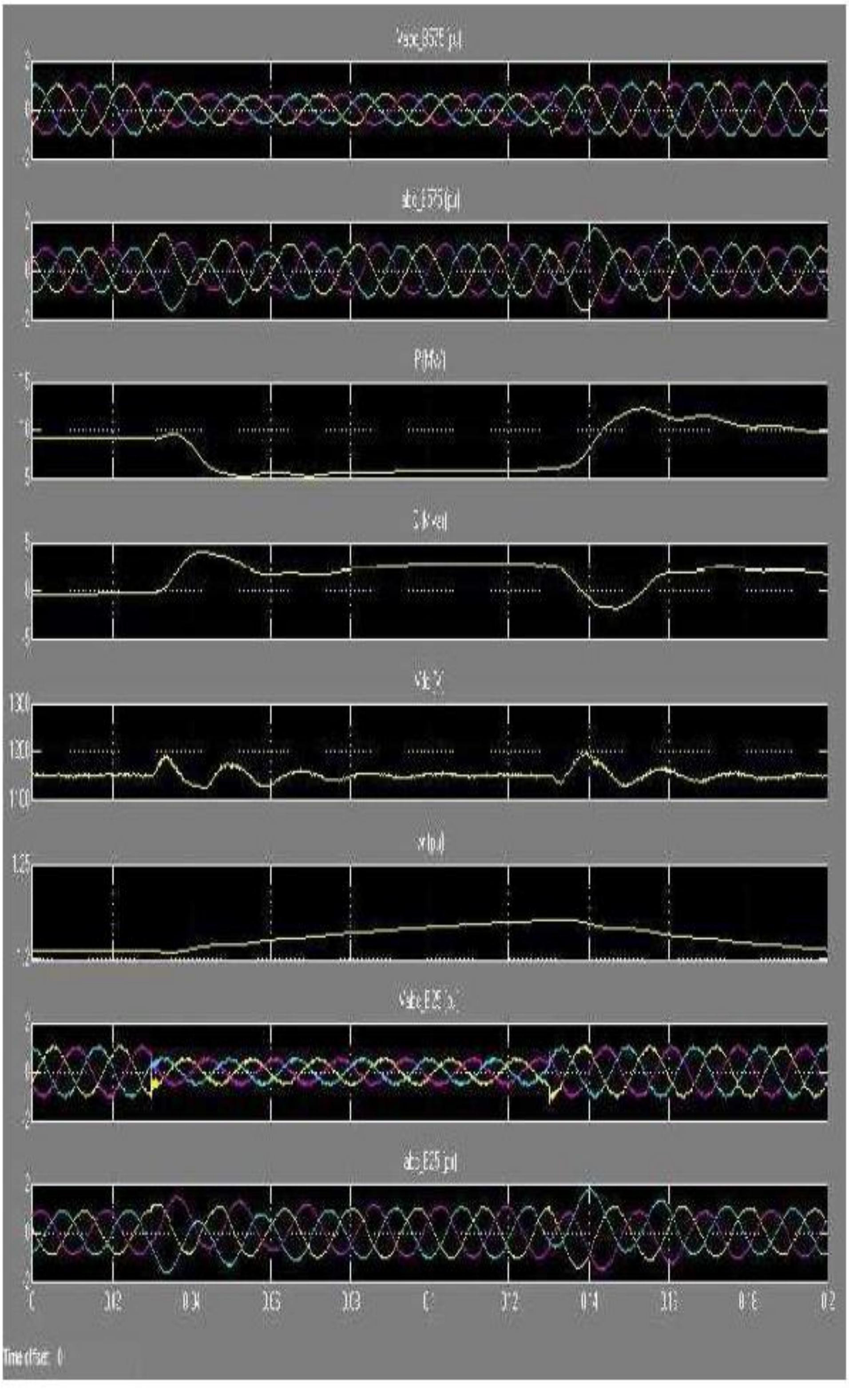

RESULT:

Thus, the MPPT tracking of DFIG were performed using MATLAB / Simulink.

SIMULATION DIAGRM:

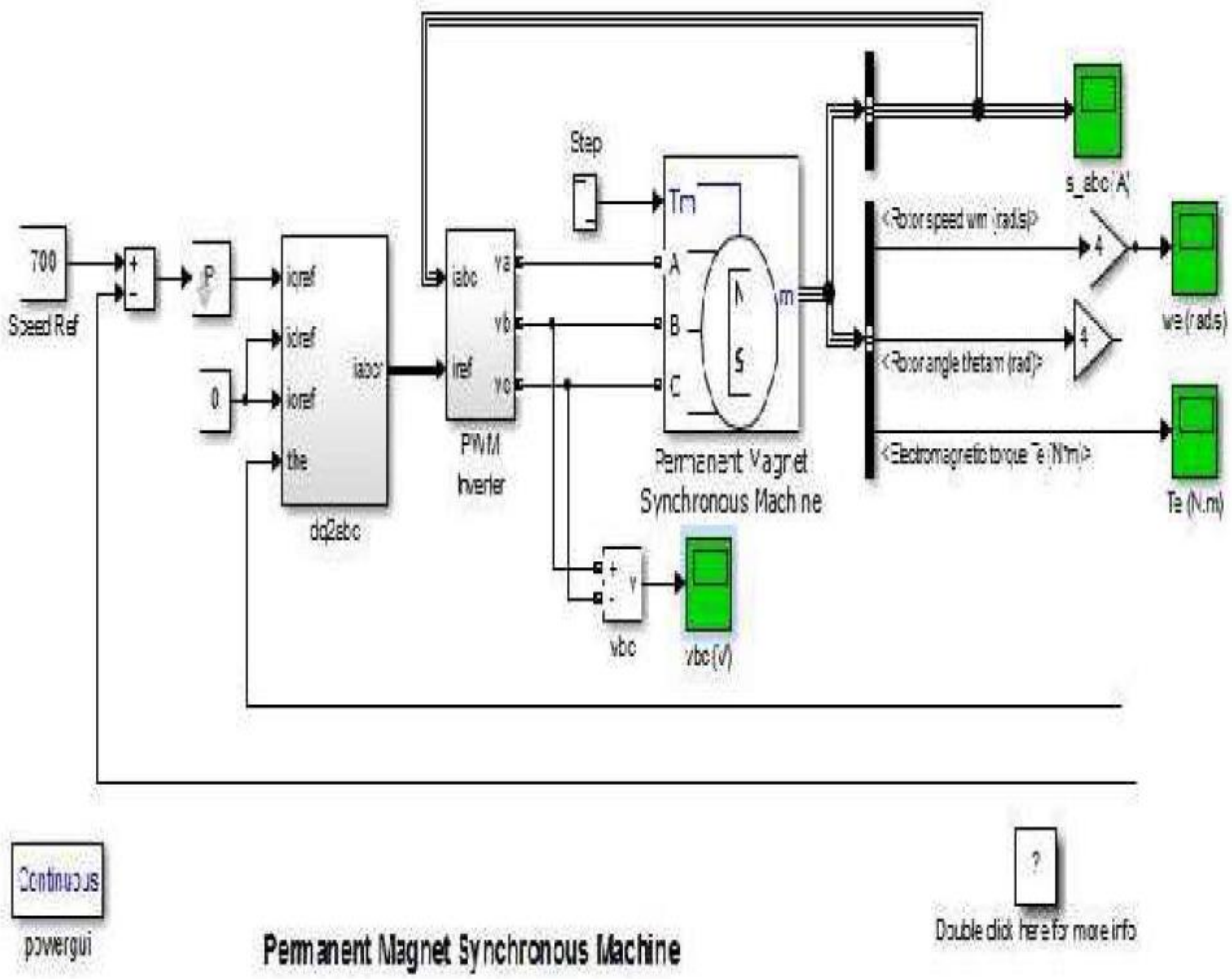

EXP.NO:8 **MPPT tracking of PMSG based WT**

DATE:

AIM:

To study MPPT tracking of PMSG based WT

THEORY:

Sustainability is the main aspect that forces the renewable energy sources to be implemented for electric energy generation instead of fossil ones. Wind energy is quite attractive among other sources because of its commercial potential [72 TW] that is five times higher than world energy demand in all forms. However, the installed capacity in 2009 was only 159GW. Large turbines play a main role on the market, but there is also demand for small turbines in the power range up to 11 kW as the power source for micro generators. Micro generator is an electrical energy source that includes all interface units and operates in parallel with the distribution network.

Current rating of such devices is limited up to 16 A per phase. Some energy sources can be connected directly to the distribution network, but in the case of DC power sources or variable speed wind turbine (VSWT) systems it is necessary to use a power converter that interfaces the source and the grid.VSWT based micro generators consist of a wind turbine, a generator and an inverter. Wind turbines capture wind energy and convert it to rotational mechanical energy. Variable speed operation of the wind turbine allows extraction of higher energy from wind than constant speed systems. The generator converts mechanical energy into electricity. Different types of generators can be used in wind energy conversion systems (WECS), but permanent magnet synchronous generators (PMSG) play a main role on the market. The main advantage of PMSG is the possibility of multipole design that offers slow speed operation and the possibility of gearless WECS construction. Another advantage is maintenance free operation since there are no brushes. The main drawback of PMSG is the dependence of its output voltage on the rotation speed. The difference between the minimum and the maximum voltage can reach four times in VSWT applications.

This drawback can be easily overcome with the help of an appropriate interfacing converter.The interfacing converter rectifies the input AC with variable voltage and frequency, adjusts voltage levels and inverts DC voltage into AC with grid voltage and frequency. Additionally, it should have maximum power point tracking (MPPT) functionality to extract more power from wind.The new topology of the interfacing converter with the HF isolation transformer for PMSG based VSWT system is presented in this paper. The topology presented has good voltage regulation capabilities at a relatively simple power circuit.

DIFFERENT TOPOLOGIES INTERFACING CONVERTER FOR WIND TURBINE.

Basically they can be divided into two groups: topologies without galvanic isolation (Fig. 1a) and those with isolation. Line frequency (LF) transformers (Fig. 1b) were widely used for galvanic isolation in last decades.Main drawbacks of LF transformer are high weight and high price. For these reasons topologies with HF isolation (Fig. 1c) have became popular especially for photovoltaic applications and wind power applications.

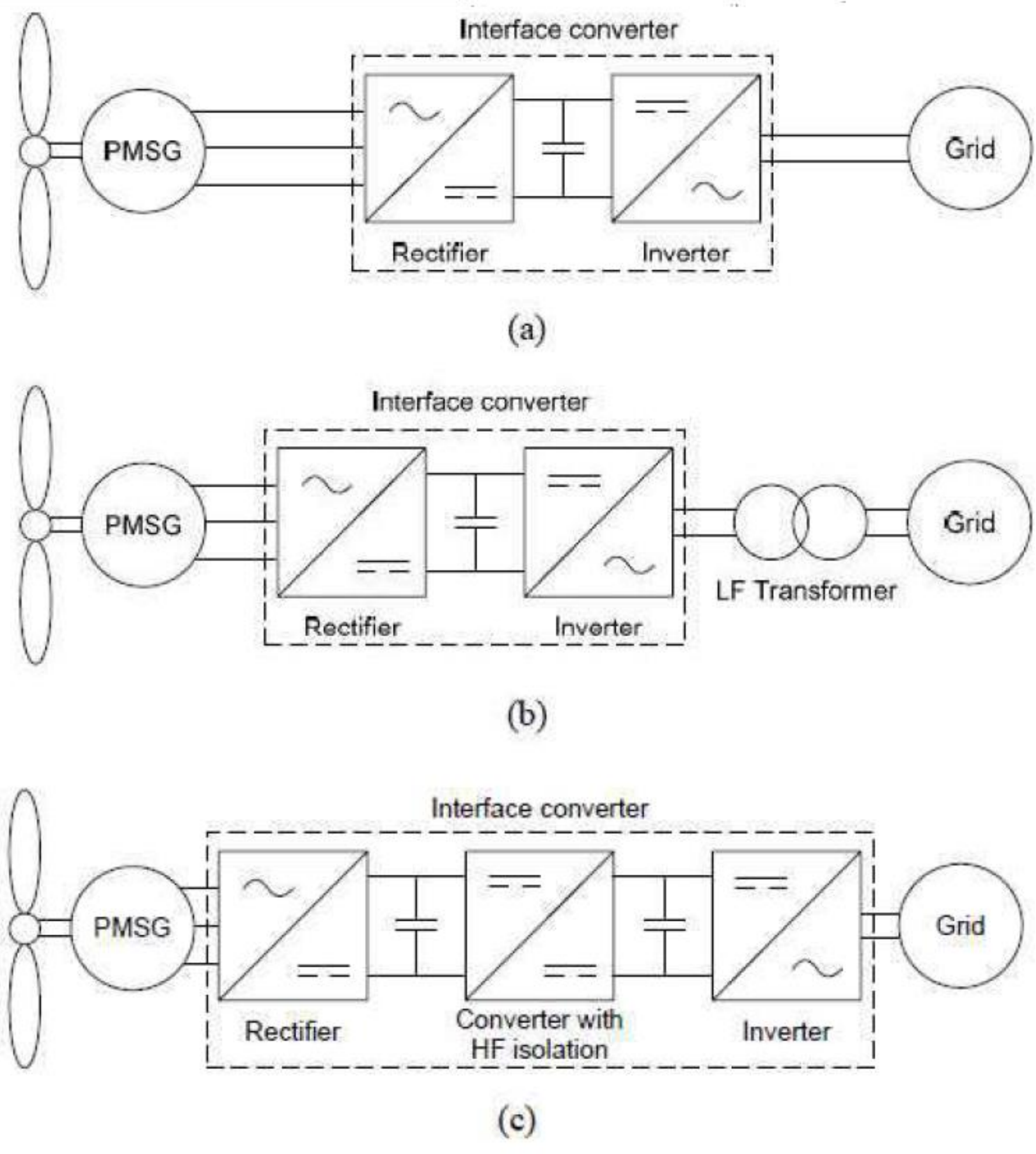

Fig 1:Block diagram of interfacing converters

TYPES OF WIND MACHINES

There are two types of wind machines (turbines) used today based on the direction of the rotating shaft (axis): horizontal–axis wind machines and vertical-axis wind machines. The size of wind machines varies widely. Small turbines used to power a single home or business may have a capacity of less than 100 kilowatts. Some large commercial sized turbines may have a capacity of 5 million watts, or 5 megawatts. Larger turbines are often grouped together into wind farms that provide power to the electrical grid.

HORIZONTAL AXIS WIND MACHINE

Most wind machines being used today are the horizontal-axis type. Horizontal-axis wind machines have blades like airplane propellers. A typical horizontal wind machine stands as tall as a 20-story building and has three blades that span 200 feet across. The largest wind machines in the world have blades longer than a football field! Wind machines stand tall and wide to capture more wind.

VERTICAL AXIS WIND MACHINE

Vertical–axis wind machines have blades that go from top to bottom and the most common type (Darrieus wind turbine) looks like a giant two-bladed egg beaters. The type of vertical wind machine typically stands 100 feet tall and 50 feet wide. Vertical-axis wind machines make up only a very small percent of the wind machines used today.

The Wind Amplified Rotor Platform (WARP) is a different kind of wind system that is designed to be more efficient and use less land than wind machines in use today. The WARP does not use large blades; instead, it looks like a stack of wheel rims. Each module has a pair of small, high capacity turbines mounted to both of its concave wind amplifier module channel surfaces. The concave surfaces channel wind toward the turbines, amplifying wind speeds by 50 percent or more. Eneco, the company that designed WARP, plans to market the technology to power offshore oil platforms and wireless telecommunications systems.

WIND TURBINE CHARACTERACTICS

Equation (1) gives the total power available in the wind,where A is the rotor area, ρ is the air density and v is the wind velocity.

$$P_{WIND} = 0.5A\rho v^3 \quad \ldots\ldots\ldots\ldots\ldots \quad (1)$$

Only a part of the total wind energy can be extracted. The available energy part in wind is described by the power coefficient C_p. The theoretical maximum value of this coefficient is 0.59 and it is called the Betz limit.

$$P_{turbine} = 0.5C_p\, Av^3 \quad \ldots\ldots\ldots\ldots \quad (2)$$

The practical values of Cp lie between 0.4 and 0.5 for industrial wind turbines.This power coefficient is a function of the tip-speed ratio λ. An example of this function is shown in Fig. 2. The tip-speed ratio shows the relation between the circumferential velocity of the blade tips and the wind velocity:

$$\lambda = \frac{r\Omega}{v} \quad \ldots\ldots\ldots\ldots\ldots\ldots\ldots (3)$$

where r is the rotor radius and Ω is the angular rotor speed.

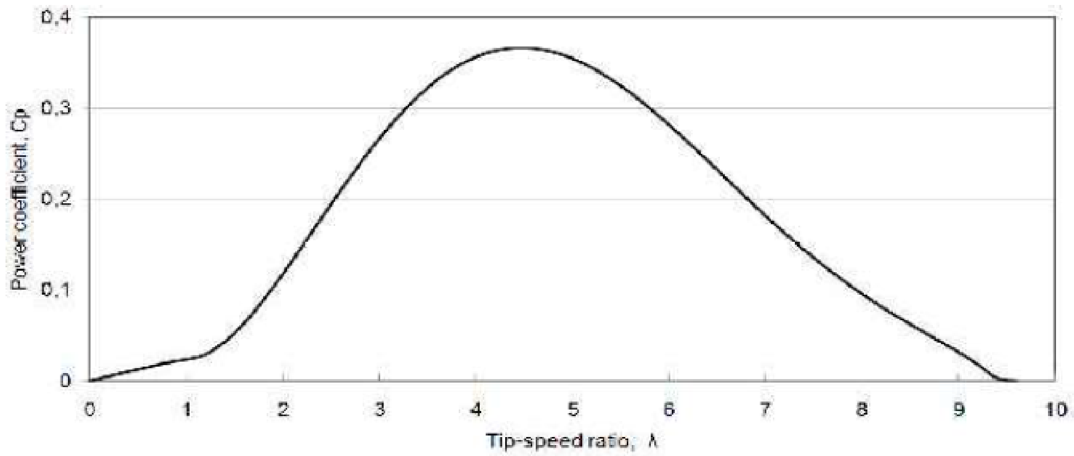

Fig. 3. Power coefficient C_p vs. tip-speed ratio.

Rotors are usually designed so that power coefficient C_p has the maximum values at the-speed ratio in the range from 4 to 8.Since the coefficient C_p is the function of the tip-speed ratio the power

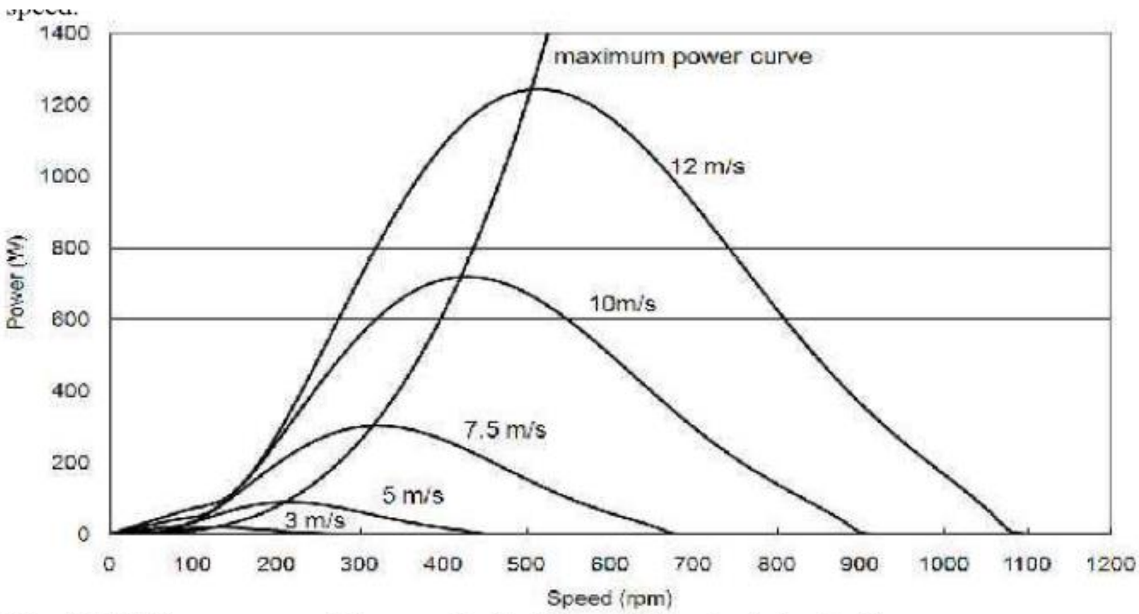

Fig. 4. VSWT power vs. rotation speed of turbine at different wind velocities.

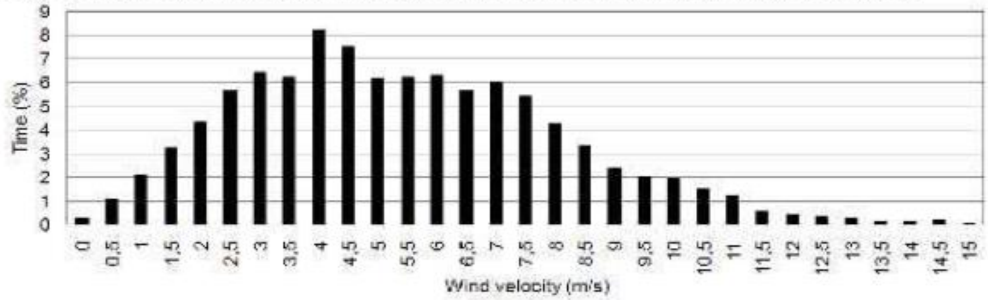

OUTPUT:

(1) is_abc(A)

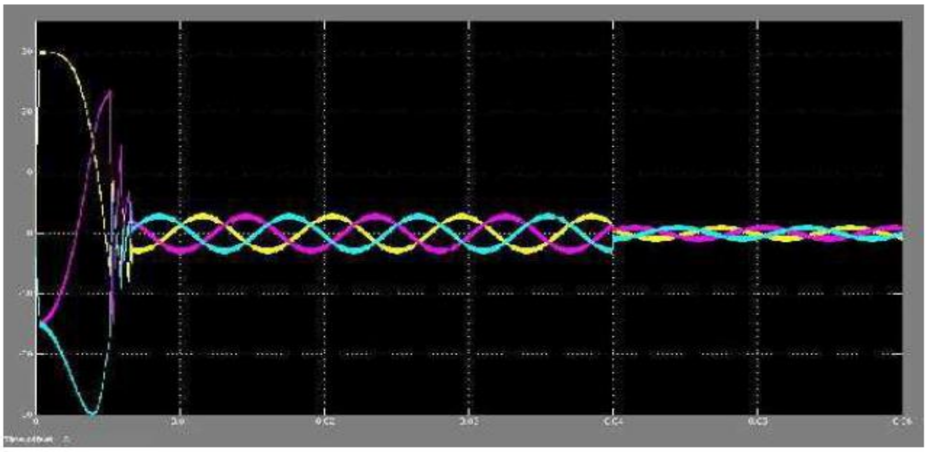

(2) we(rad/s)

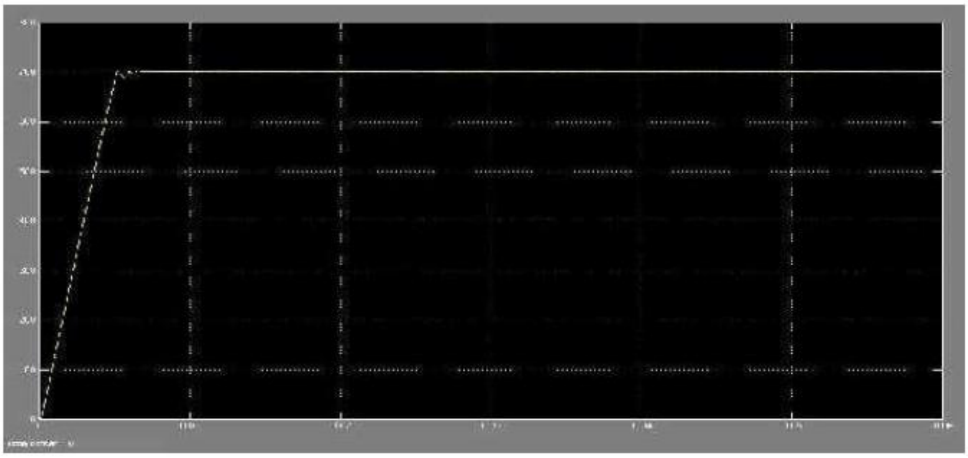

(3)Te(Nm)

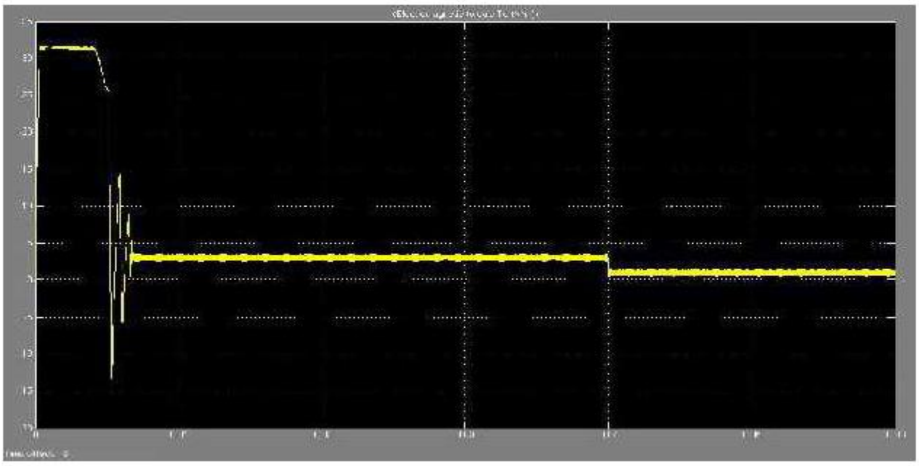

RESULT:

Thus the MPPT tracking of DFIG were studied using MATLAB / Simulink.

EXP.NO: 9 **Grid Integration of RES**

DATE :

AIM:

To conduct experiment on Performance assessment of Grid connected and Standalone 1kWp Solar Power System.

THEORY:

Standard Test Conditions (STC)

1. Temperature of the cell – 25°C. The temperature of the solar cell itself, not the temperature of the surrounding.
2. Solar Irradiance – 1000 Watts per square meter. This number refers to the amount of light energy falling on a given area at a given time.
3. Mass of the air – 1.5. This number is somewhat misleading as it refers to the amount of light that has to pass through Earth's atmosphere before it can hit Earth's surface, and has to do mostly with the angle of the sun relative to a reference point on the earth. This number is minimized when the sun is directly above as the light has to travel a minimum distance straight down, and increases as the sun goes farther from the reference point and has to go at an angle to hit the same spot.

Formula Used:

1. The specific energy yield is expressed in kWh per KWp and it calculated as follows:

   $$S_P = E_{sys} / P_{array-STC}$$

   where

   The AC energy of the solar array delivered to the grid is the Esys in the above formula while the actual STC rating of the array is P array STC.

2. The performance ratio (PR)

$$R = E_{sys} / E_{ideal}$$

where

E sys - actual yearly energy yield from the system

E ideal- the ideal energy output of the array.

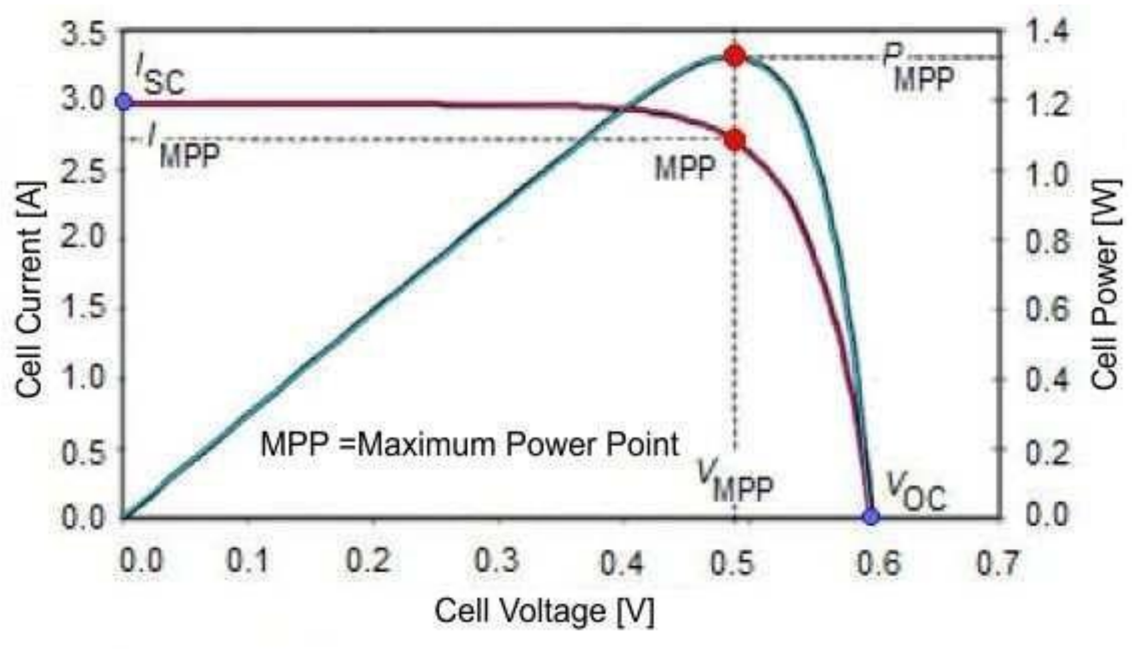

I-V Characteristics of PV System

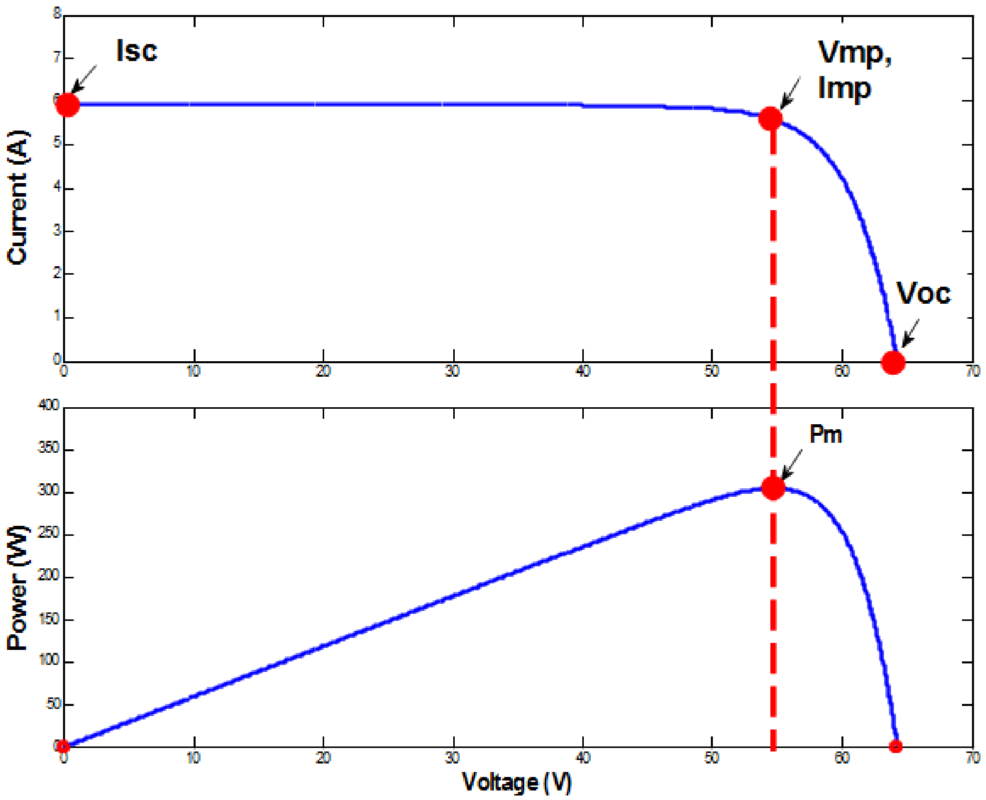

Power Vs Voltage and Current Characteristics.

SIMULATION DIAGRAM:

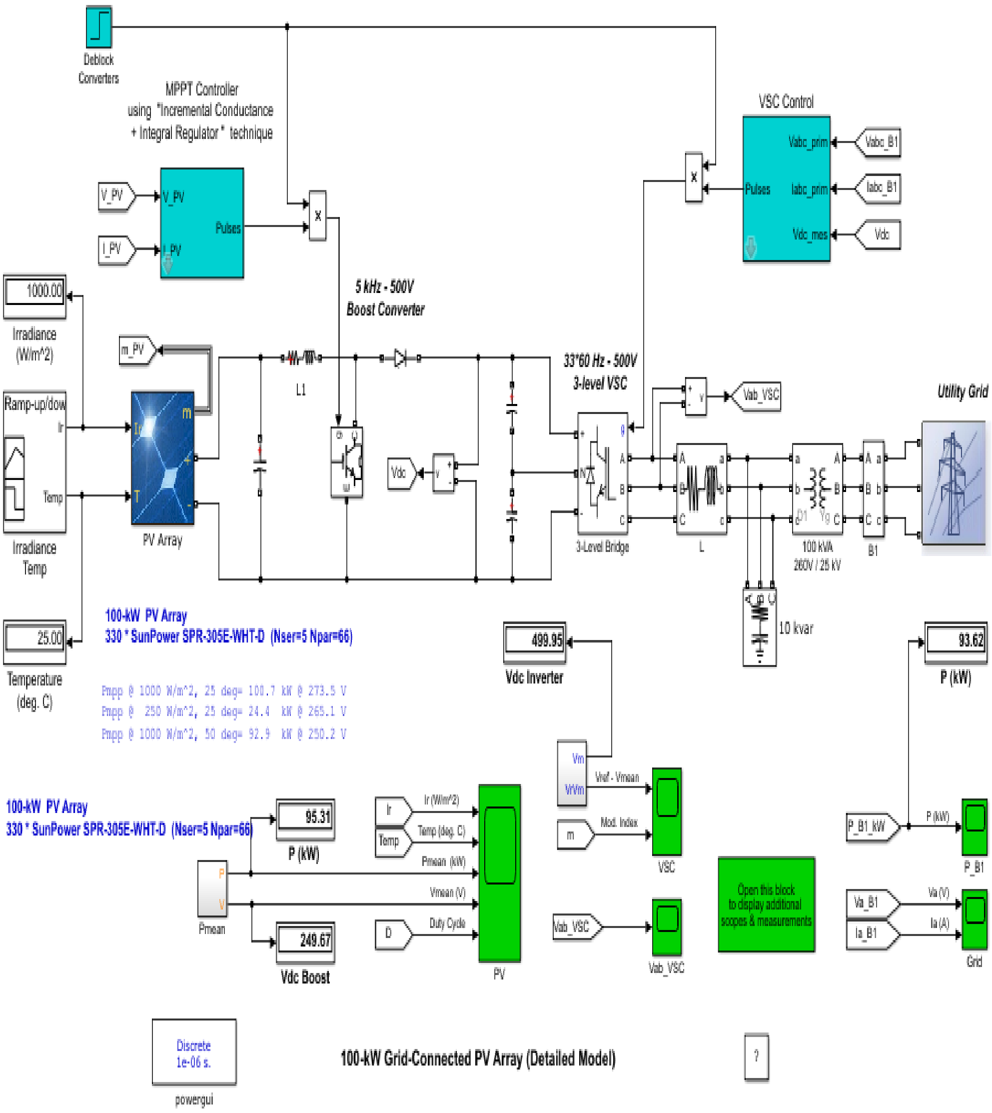

OUTPUT:

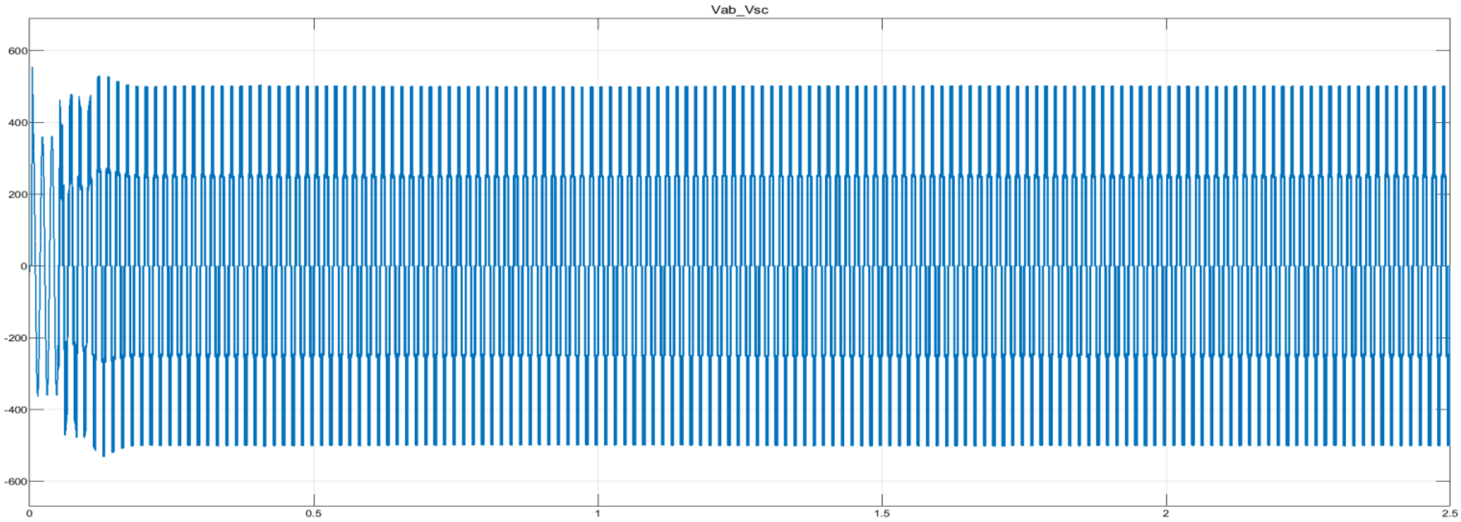
Vab_Vsc
600
400
200
0
-200
-400
-600
0
0.5
1
1.5
2
2.5

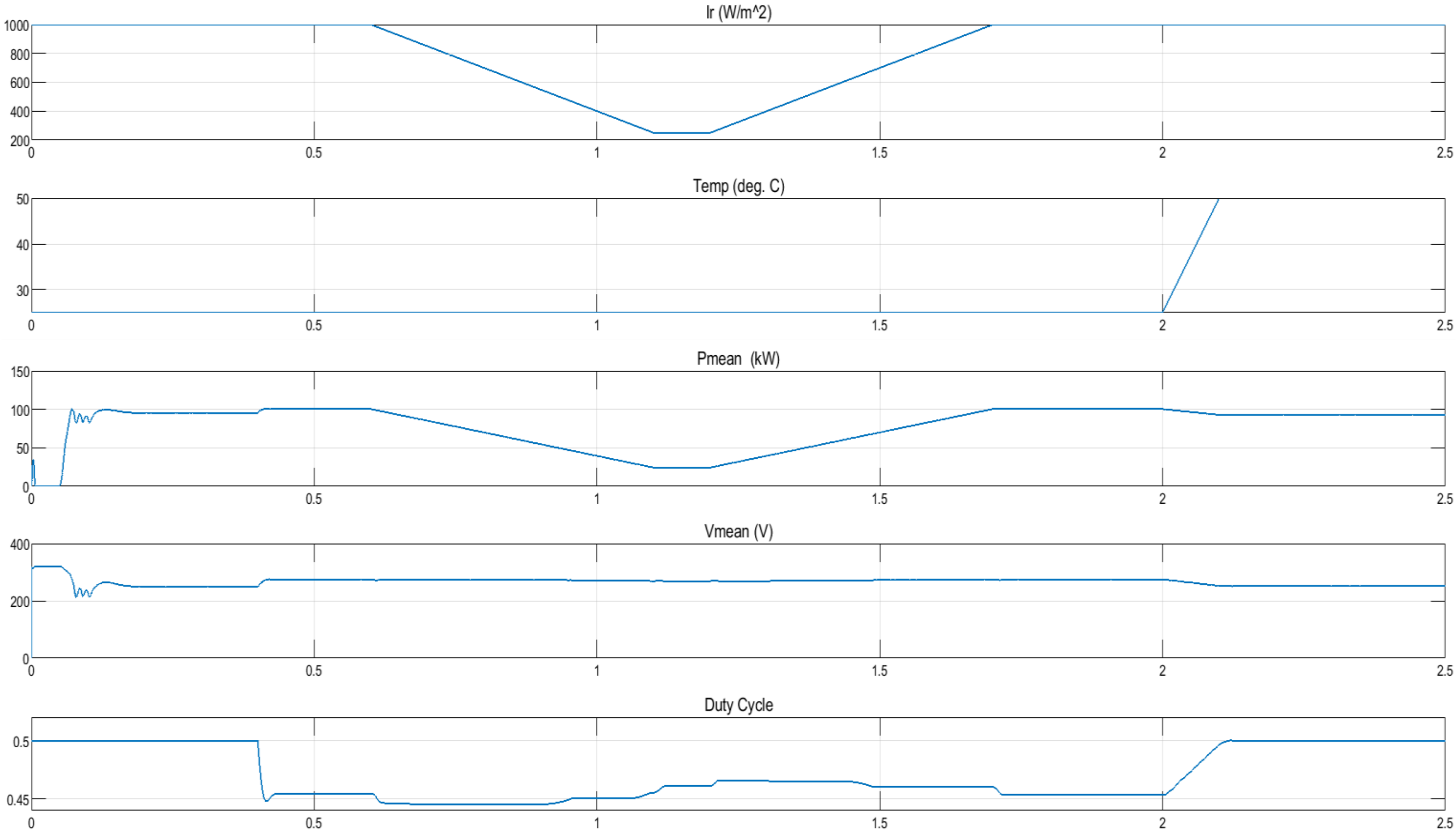
Ir (W/m^2)
1000
800
600
400
200
Temp (deg. C)
50
40
30
Pmean (kW)
150
100
50
0
Vmean (V)
400
200
0
Duty Cycle
0.5
0.45
0
0.5
1
1.5
2
2.5

RESULT:

Thus, the experiment on performance assessment of grid connected and standalone 1kWp solar power system was performed using MATLAB simulink.

EXP.NO: 10 **Modeling of Active filter for Power system**

DATE:

AIM:

To design the active filter to improve power quality by mitigation harmonics**.**

THEORY:

As the development of modern power electronics technology and the wider application of various nonlinear devices, the current distortion makes increasingly serious pollution to the grid. Therefore, harmonic current compensation has been drawn great attention.Active power filter is a new type of power electronic device using for dynamic suppressing harmonics and compensating reactive power. It can compensate harmonics with varying amplitude and frequency, and can overcome the shortage of passive filter effectively. It is a harmonics suppression device with prospect .

PRINCIPLE AND STRUCTURE:

The structure of a shunt active power filter used for three-phase four-wire is shown in Fig. 1. In this system, the load may product harmonics and unbalance current in three-phase, and current is flown in neutral wire.

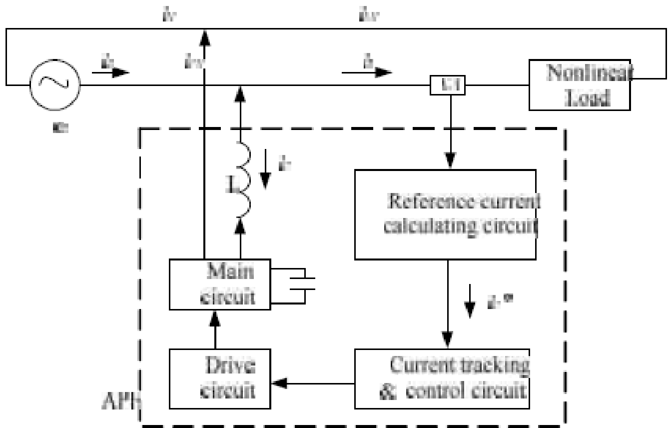

Fig. 1: The structure of active power filter for three-phase four-wire system

The shunt active power filter is a voltage source inverter controlled as a current source by means of pulse width modulation signals. As it can be seen in Fig. 1, the filter is connected in paralleled with the nonlinear load. Harmonic current compensation is achieved by injecting equal but opposite harmonic current components at the point of connection, therefore canceling the original distortion and improving the power quality . In most cases, the load also needs reactive power, which can also be generated by the same current source. In three-phase unbalanced and nonlinear loads, it is also possible to redistribute power and to keep the system balance. The active power filter is composed of the reference current calculating circuit, current tracking circuit, driving circuit and the main circuit. While, the generation circuit of compensating current is composed of the last three parts Three-phase four-wire system is different from three-phase three-wire system because of the neutral wire. Thus, handling zero-sequence components of three-phase current is the key point. Reference current calculating circuit should product the reference current correctly and fast in three-phase four-wire system. That means it should detect the harmonics, fundamental negative-sequence current components and zero-sequence current components of the compensating . The generation circuit of compensating current should product compensating current correctly according to the reference current signals.

Because the sum of three-phase current is not zero in three-phase four-wire system, the detection method based on instantaneous reactive power theory should be modified. The way is to calculate the zero-sequence current components, then subtract them from three-phase current. Finally three-phase current without zero-sequence components can be detected by the method based on instantaneous reactive power theory. The compensating current signals of the neutral wire can be also calculated by turning the polarity of the neutral wire current over . The principle of reference current calculating circuit is shown in Fig. 2. In which, i_a, i_b, i_c are load currents. The zero-sequence component of three-phase current i_n is calculated as:

$$i_n = \frac{1}{3}(i_a + i_b + i_c) \qquad (1)$$

Then zero-sequence components can be subtracted from three-phase current:

$$\begin{aligned} i_a' &= i_a - i_n \\ i_b' &= i_b - i_n \qquad (2) \\ i_c' &= i_c - i_n \end{aligned}$$

Eventually the three-phase currents without zero-sequence component i_a', i_b', i_c' will comply with:

$$i_a' + i_b' + i_c' = 0 \qquad (3)$$

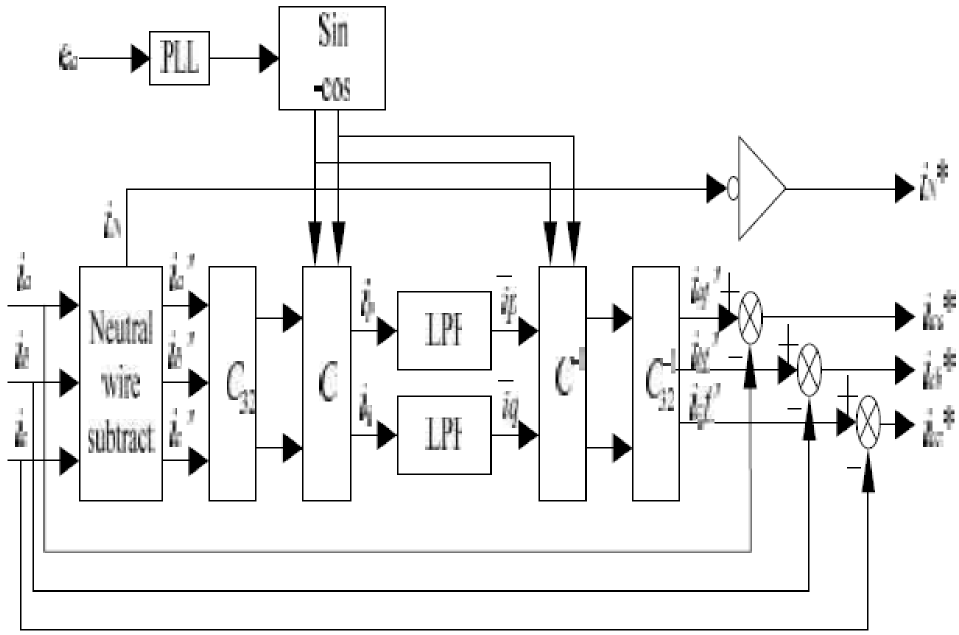

Fig. 2: The principle diagram of reference current calculating circuit

Afterward, as shown in Fig. 2, the three-phase currents without zero-sequence components $i_a^{'}, i_b^{'}, i_c^{'}$ are coordinately transformed and achieve corresponding active power current component i_p and reactive power current component i_q, then it can acquire dc component $\overline{i_p}, \overline{i_q}$ through the low pass filters. Fundamental positive-sequence components $i_{af}^{'}, i_{bf}^{'}, i_{cf}^{'}$ can be calculated by inverse coordinate transformation. When the positive-sequence components are subtracted from load current i_a, i_b, i_c, there will be reference current $i_{ca}^*, i_{cb}^*, i_{cc}^*$. After the compensating currents generated by the reference signals offset the harmonics, the currents flowing into source which are equal to fundamental positive-sequence components are sinusoid and balanced

Design of Shunt Active Power Filter

Active power filter is an advanced power electronic device, which can be used for integrated compensating harmonics, reactive currents and negative-sequence currents. Because of the characteristics of real time and accurate compensation, it is possible to take full advantage of digital signal processing and many other technologies. If so, the performance of active power filters can be improved significantly.

Control circuit

The control circuit consists of current control and voltage control. The principle is shown in Fig. 3. The current controller uses the current error between reference current i_c^* and compensating current i_c filtered by a proportional-integral regulator as the modulating signal. The current control circuit uses a tracking PWM current control and timing comparing. The comparator is judged at each clock-cycle, so the PWM control signals change once at least one clock cycle. The clock-cycle limits the highest frequency of switching devices in the main circuit, thus damages to the devices due to over-high switching frequency may be avoided. The shortcoming of this control method is that the tracking error of compensating current is unfixed .

For voltage control, it mainly means controlling of DC-link voltage. There are two control techniques: PI control and fuzzy control. PI control is similar to the current control, but there is some difference. When the supply voltage is unbalanced or distorted, the input of the voltage controller is not the actual supply voltage but a unitary sinusoidal waveform in phase with the supply voltage . Therefore, the active power filter will have good performance even under the condition of unbalanced or distorted source voltage. In other words, PI control uses the voltage error between DC-link voltage and its reference filtered by a proportional-integral regulator multiplied by the unitary sinusoidal waveform in phase with the supply voltage to obtain the reference current.

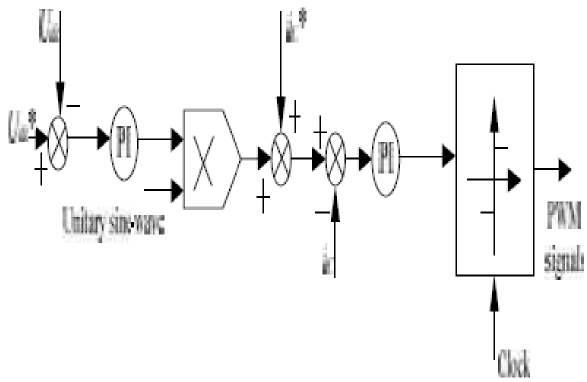

fig. 3: The principle diagram of control circuit

Simulation circuit:

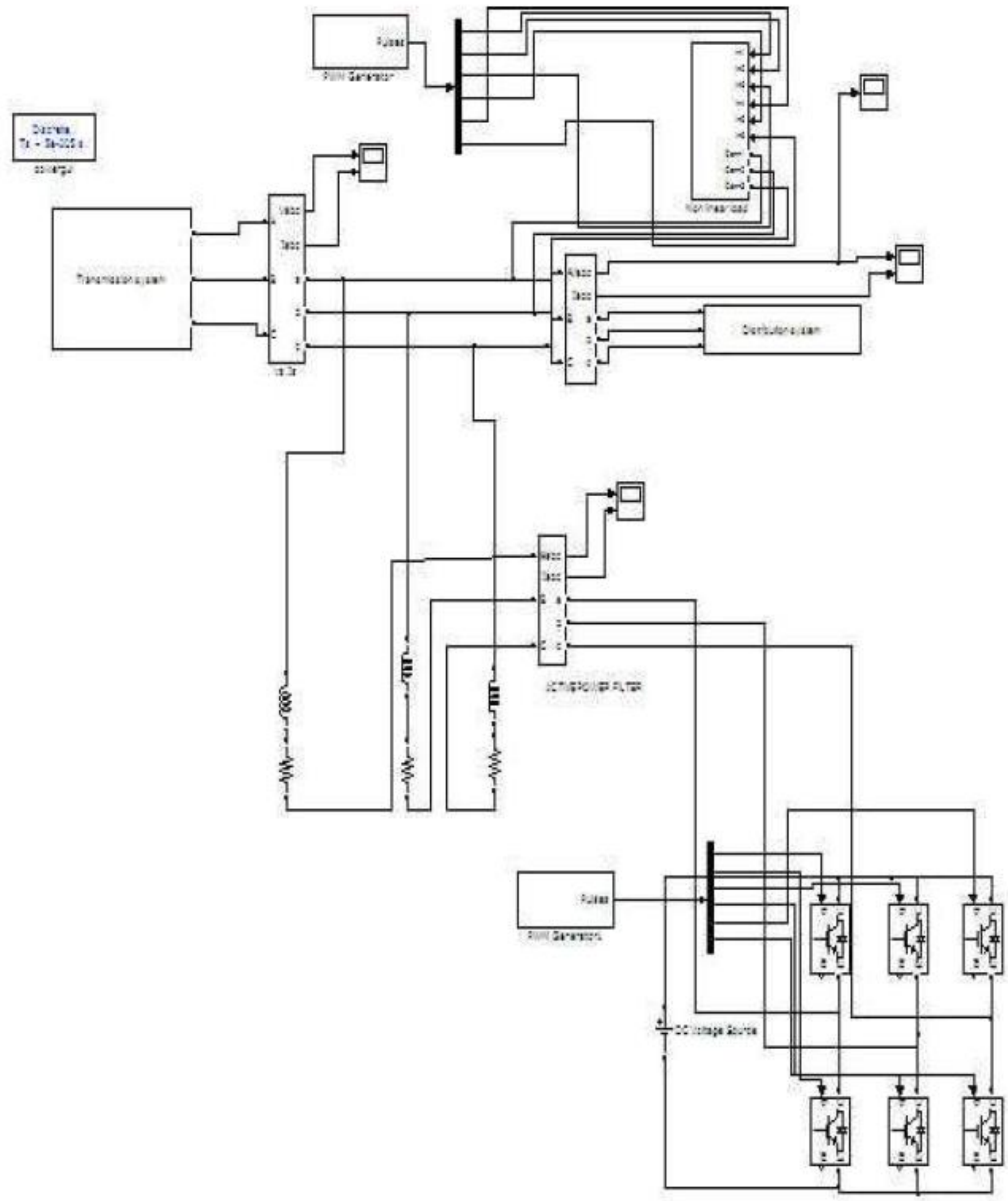

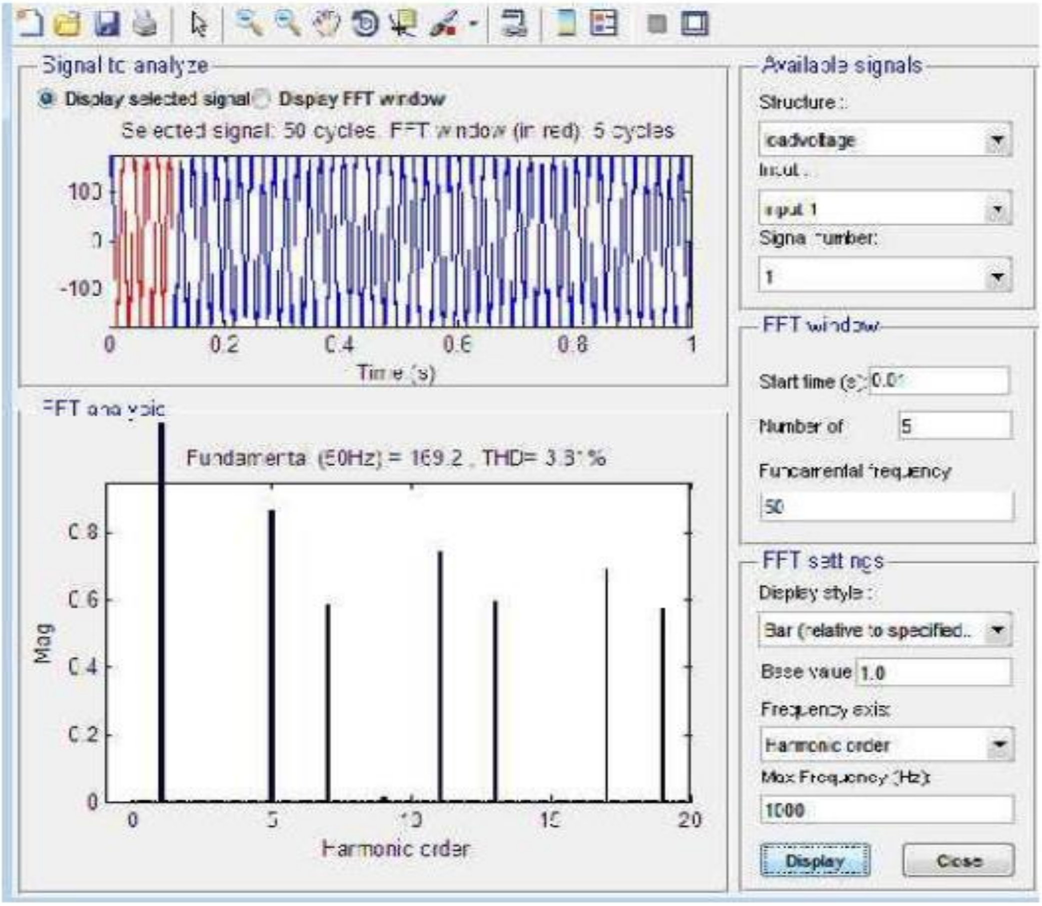

Simulation outputs

RESULT:

Thus, the active filter to improve power quality by mitigation harmonics were studied.

Simulation diagram:

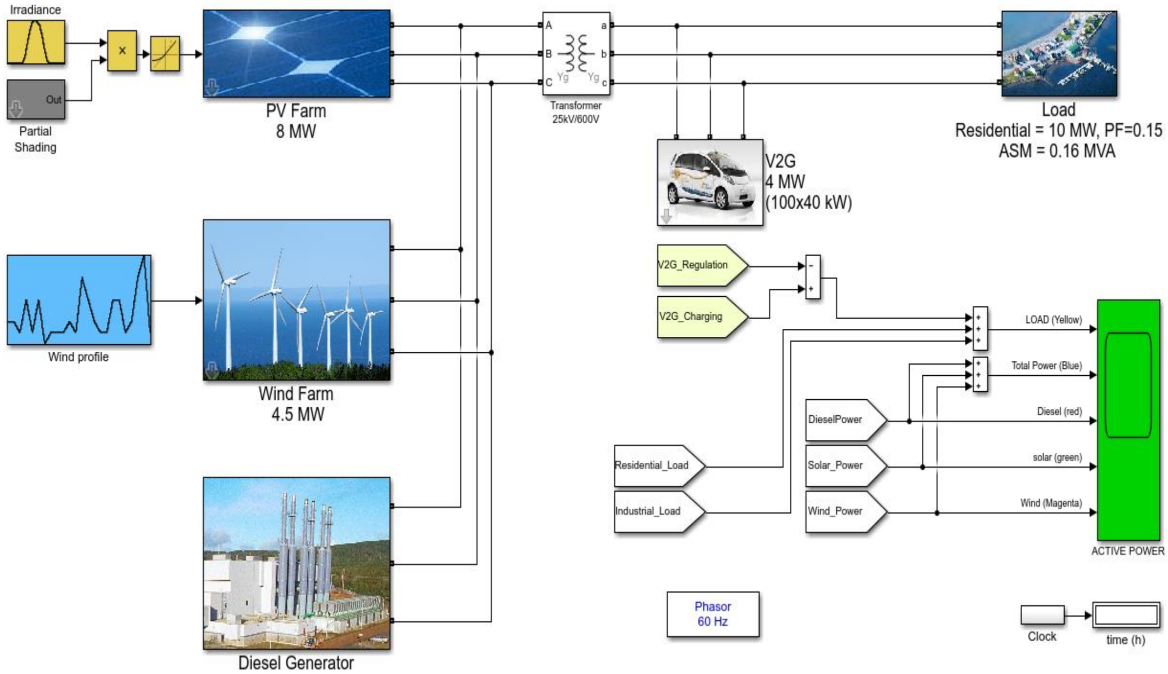

EXP.NO: 11 Simulation study on Hybrid (Solar-Wind) Power System

DATE:

AIM:

To study the simulation of Hybrid (Solar-Wind) Power System.

THEORY:

The Solar PV wind hybrid system suits to conditions where sunlight and wind has seasonal shifts . As the wind does not blow throughout the day and the sun does not shine for the entire day, using a single source will not be a suitable choice. A hybrid arrangement of combining the power harnessed from both the wind and the sun and stored in a battery can be a much more reliable and realistic power source. The load can still be powered using the stored energy in the batteries even when there is no sun or wind.

PV and wind system, both depending on weather condition, individual hybrid PV and hybrid wind system does not produce usable energy throughout the year. For better performance of the standalone individual PV combination or wind combination need battery backup unit and diesel generator set, which increase the hybrid system cost for proper operation and better reliability, and lower cost of the system, studies are reported by researchers regarding the combination of hybrid PV–wind system.

PROCEDURE:

1. Matlab Simulink model file is created.
2. Simulink library used to generate required components.
3. Scope is used to view results for different conditions of shadowing.

Description:

The micro grid is divided into four important parts: A diesel generator, acting as the base power generator; A PV farm combined with a wind farm, to produce renewable energy; a V2G system installed next to the last part of the system which is the load of the grid. The size of the micro grid represents approximately a community of a thousand households during a low consumption day in spring or fall. There are 100 electric vehicles in the base model which means that there is a 1:10 ratio between the cars and the households. This is a possible scenario in a foreseeable future.

Load:

The load is composed of residential load and an asynchronous machine that is used to represents the impact of an industrial inductive load (like a ventilation system) on the micro grid. The residential load follows a consumption profile with a given power factor. The asynchronous machine is controlled by a square relation between the rotor speed and the mechanical torque.

Combined solar and wind system model:

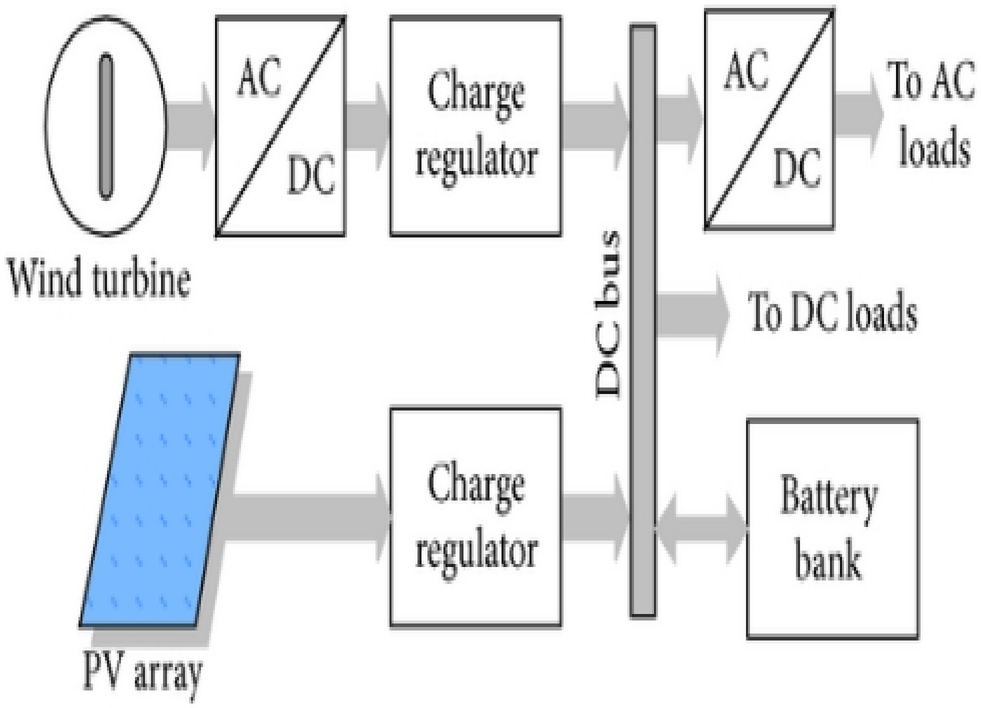

WIND TURBINE OUTPUT:

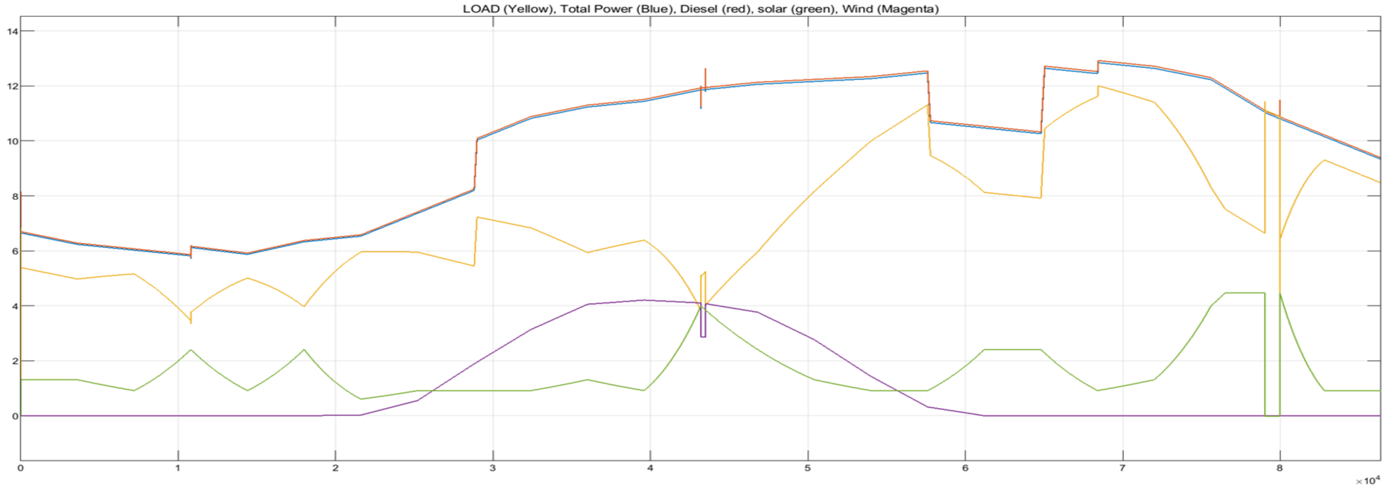

RESULT:

Thus the simulation of Hybrid (Solar-Wind) Power System were performed.

EXP.NO: 12 Simulation study on Intelligent Controllers for Hybrid Systems.

DATE:

AIM:

To study the simulation of intelligent controllers for a Stand-Alone Hybrid Generation System.

THEORY:

The study aims at the modeling and power flow analysis of a stand-alone hybrid generating system (SAHGS) comprising of wind and photovoltaic systems. The wind driven self-excited induction generator (SEIG), photovoltaic array and other network components are modeled and simulated using Matlab/Simulink. The variable voltage and frequency of a generator is first rectified and controlled by a DC/DC converter before being fed to a common DC bus.

The variable output voltage of the photovoltaic module is also controlled by a DC/DC converter. The DC bus collects the total power from the wind and photovoltaic systems and uses it partly to supply the required load demand and partly to charge the battery bank. The individual systems are simulated for varying wind velocities and solar intensities respectively and the results are used to identify the operating modes. A neuro controller is designed to adjust the duty ratios of the choppers and the firing angle of the converter at which the maximum power generation occurs.

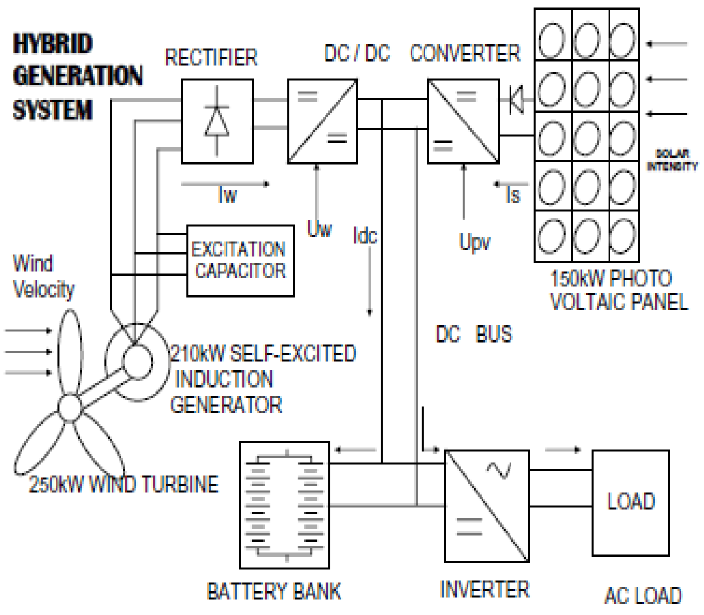

Fig. 1. Schematic Representation of a Hybrid Generation System.

The SAHGS considered for study is a combination of the wind and photovoltaic systems as shown in Fig. 1. The wind system houses a 250kW wind turbine that converts the kinetic energy present in the wind into mechanical energy, which drives the 210kW self–excited induction generator through a gear box. Since the wind is an intermittent source of energy, the output voltage and frequency from the generator will vary for different wind velocities.

The variable output ac power from the generator is first converted into dc using an uncontrolled diode bridge rectifier. A buck chopper is used to match the variable DC voltage with the DC bus. The voltage across the rectifier terminal is controlled by varying the duty ratio of the DC/DC converter before it is fed to the DC bus.

The photovoltaic panel is built up of a combination of series and parallel individual photovoltaic modules. As the solar intensity varies, the DC output voltage of the panel also varies. This variable DC output voltage of the panel is controlled by another DC/DC converter before it is fed to the DC bus. The common DC bus collects the total energy from the wind and the photovoltaic systems and uses it partly to supply the required load demand and partly to charge the battery bank. Under normal operating conditions of wind velocity and solar intensity, the battery bank is an additional load to the system. It acts as an additional source to supply the demand during low wind velocities or solar intensities.

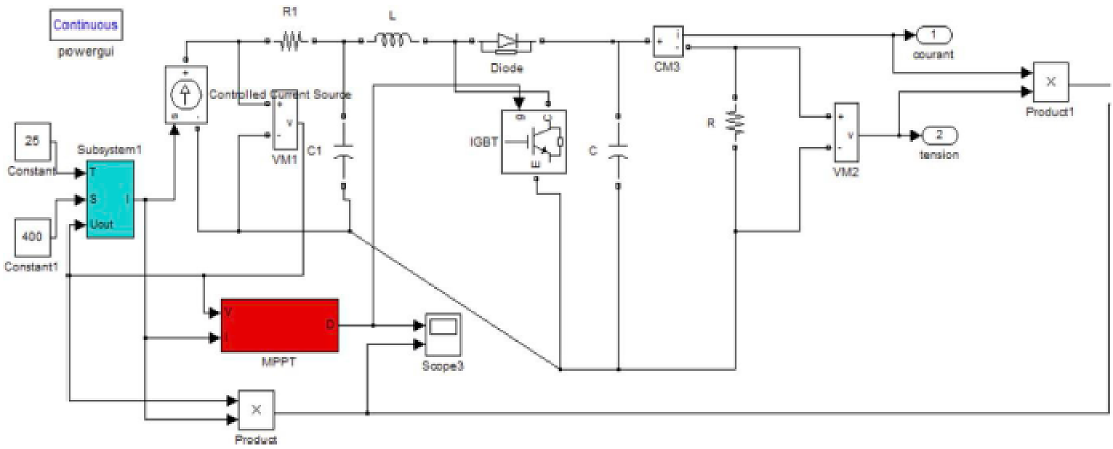

Fig.2.Model of the PV system developed under Matlab-Simulink

Response of the Neuro Controller

The neuro controller uses the wind velocity and the solar intensity as the input signals. The output of the controller are the duty ratios of the chopper and the firing angle of the controlled rectifier .Fig. 3. Simulation results of the PV system for varying cell temperatures.
The network architecture illustrated in Fig. is included in the SAHGS model for simulation. It is trained with about 150 simulation data using back propagation algorithm. The response of the controller for individual and simultaneous changes in both the wind velocity and the solar intensity are shown in Fig.3. It is observed that for every wind velocity and cell temperature, the neuro controller automatically outputs the corresponding duty ratios of the choppers and the firing angle of the controlled rectifier respectively so as to extract maximum power and also to maintain the DC bus voltage constant.

The dynamic model of a hybrid generating system comprising a wind driven self-excited induction generator , photovoltaic system and the power conditioning circuit (uncontrolled rectifier –buck chopper) is developed. The individual system performance of the wind and PV systems are studied through simulation for varying wind velocities and solar intensities respectively .From the simulation results, the optimum value of excitation capacitance and number of battery are identified. It is found that the power generation increases with decreasing duty ratio (in turn the input voltage to the chopper) and the maximum generationis found to be 92 kW at dw =0.1 and 150kW at dPV =0.13 respectively . A further reduction in dc voltage is obtained by using a controlled rectifier and improvement in power generation is found to be about 17 percent of rated value. The simulation is repeated for varying wind velocities and the optimum value of alpha and duty ratio are found. Similar analysis is carried out for the solar system also and the optimum duty ratio is found for different cell temperatures. The neuro controller designed for the automatic variation of dw, dPV and alpha exhibits an excellent dynamic response.

RESULT:

Thus, the study of simulation of intelligent controllers for a Stand-Alone Hybrid Generation System has been done.